CHARACTERIZING LOOKAHEAD DYNAMICS OF SMOOTH GAMES

Anonymous authors
Paper under double-blind review

ABSTRACT

As multi-agent systems proliferate in machine learning research, games have attracted much attention as a framework to understand optimization of multiple interacting objectives. However, a key challenge in game optimization is that, in general, there is no guarantee for usual gradient-based methods to converge to a local solution of the game. The latest work by Chavdarova et al. (2020) report that Lookahead optimizer (Zhang et al., 2019) significantly improves the performance of Generative Adversarial Networks (GANs) and reduces the rotational force of bilinear games. While promising, their observations were purely empirical, and Lookahead optimization of smooth games still lacks theoretical understanding. In this paper, we fill this gap by theoretically characterizing Lookahead dynamics of smooth games. We provide an intuitive geometric explanation on how and when Lookahead can improve game dynamics in terms of stability and convergence. Furthermore, we present sufficient conditions under which Lookahead optimization of bilinear games provably stabilizes or accelerates convergence to a Nash equilibrium of the game. Finally, we show that Lookahead optimizer preserves locally asymptotically stable equilibria of base dynamics, and can either stabilize or accelerate the local convergence to a given equilibrium with proper assumptions. We verify our theoretical predictions by conducting numerical experiments on two-player zero-sum (non-linear) games.

1 INTRODUCTION

Recently, a plethora of learning problems have been formulated as games between multiple interacting agents, including Generative Adversarial Networks (GANs) (Goodfellow et al., 2014; Brock et al., 2019; Karras et al., 2019), adversarial training (Goodfellow et al., 2015; Madry et al., 2018), self-play (Silver et al., 2018; Bansal et al., 2018), inverse reinforcement learning (RL) (Fu et al., 2018) and multi-agent RL (Lanctot et al., 2017; Vinyals et al., 2019). However, the optimization of interdependent objectives is a non-trivial problem, in terms of both computational complexity (Daskalakis et al., 2006; Chen et al., 2009) and convergence to an equilibrium (Goodfellow, 2017; Mertikopoulos et al., 2018; Mescheder et al., 2018; Hsieh et al., 2020). In particular, gradient-based optimization methods often fail to converge and oscillate around a (local) Nash equilibrium of the game even in a very simple setting (Mescheder et al., 2018; Daskalakis et al., 2018; Mertikopoulos et al., 2019; Gidel et al., 2019b;a). To tackle such non-convergent game dynamics, a huge effort has been devoted to developing efficient optimization methods with nice convergence guarantees in smooth games (Mescheder et al., 2017; 2018; Daskalakis et al., 2018; Balduzzi et al., 2018; Gidel et al., 2019b;a; Schäfer & Anandkumar, 2019; Yazici et al., 2019; Loizou et al., 2020).

Meanwhile, Chavdarova et al. (2020) have recently reported that the Lookahead optimizer (Zhang et al., 2019) significantly improves the empirical performance of GANs and reduces the rotational force of a bilinear game dynamics. Specifically, they demonstrate that class-unconditional GANs trained by a Lookahead optimizer can outperform class-conditional BigGAN (Brock et al., 2019) trained by Adam (Kingma & Ba, 2015) even with a model of $1/30$ parameters and negligible computation overheads. They also show that Lookahead optimization of a stochastic bilinear game tends to be more robust against large gradient variances than other popular first-order methods, and converges to a Nash equilibrium of the game where other methods fail.

Despite its great promise, the study of Chavdarova et al. (2020) relied on purely empirical observations, and the dynamics of Lookahead game optimization still lacks theoretical understanding. Specifically, many open questions, such as the convergence properties of Lookahead dynamics and the impact of its hyperparameters on the convergence, remain unexplained. In this work, we fill this gap by theoretically characterizing the Lookahead dynamics of smooth games. Our contributions are summarized as follows:

- We provide an intuitive geometric explanation on how and when Lookahead can improve the game dynamics in terms of stability and convergence to an equilibrium.
- We analyze the convergence of Lookahead dynamics in bilinear games and present sufficient conditions under which the base dynamics can be either stabilized or accelerated.
- We characterize the limit points of Lookahead dynamics in terms of their stability and local convergence rates. Specifically, we show that Lookahead (i) preserves locally asymptotically stable equilibria of base dynamics and (ii) can either stabilize or accelerate the local convergence to a given equilibrium by carefully choosing its hyperparameters.
- Each of our theoretical predictions is verified with numerical experiments on two-player zero-sum (non-linear) smooth games.

2 PRELIMINARIES

We briefly review the objective of smooth game optimization, first-order game dynamics, and Lookahead optimizer. Finally, we discuss previous work on game optimization. We summarize the notations throughout this paper in Table A.1.

2.1 SMOOTH GAMES

Following Balduzzi et al. (2018), a smooth game between players $i = 1, \ldots, n$ can be defined as a set of smooth scalar functions $\{f_i\}_{i=1}^n$ with $f_i : \mathbb{R}^d \to \mathbb{R}$ such that $d = \sum_{i=1}^n d_i$. Each f_i represents the cost of player i's strategy $\mathbf{x}_i \in \mathbb{R}^{d_i}$ with respect to other players' strategies $\mathbf{x}_{-i}$. The goal of this game optimization is finding a (local) Nash equilibrium of the game (Nash, 1951), which is a strategy profile where no player has an unilateral incentive to change its own strategy.

Definition 1 (Nash equilibrium)**.** *Let $\{f_i\}_{i=1}^n$ be a smooth game with strategy spaces $\{\mathbb{R}^{d_i}\}_{i=1}^n$ such that $d = \sum_{i=1}^n d_i$. Then $\boldsymbol{x}^* \in \mathbb{R}^d$ is a local Nash equilibrium of the game if, for each $i = 1, \ldots, n$, there is a neighborhood U_i of $\boldsymbol{x}_i^*$ such that $f_i(\boldsymbol{x}_i, \boldsymbol{x}_{-i}^*) \geq f_i(\boldsymbol{x}^*)$ holds for any $\boldsymbol{x}_i \in U_i$. Such $\boldsymbol{x}^*$ is said to be a global Nash equilibrium of the game when $U_i = \mathbb{R}^{d_i}$ for each $i = 1, \ldots, n$.*

A straightforward computational approach to find a (local) Nash equilibrium of a smooth game is to carefully design a gradient-based strategy update rule for each player. Such update rules that define iterative *plays* between players are referred to as a *dynamics* of the game.

Definition 2 (Dynamics of a game)**.** *A dynamics of a smooth game $\{f_i\}_{i=1}^n$ indicates a differentiable operator $F : \mathbb{R}^d \to \mathbb{R}^d$ that describes players' iterative strategy updates as $\boldsymbol{x}^{(t+1)} = F(\boldsymbol{x}^{(t)})$.*

One might expect that a simple myopic game dynamics, such as gradient descent, would suffice to find a (local) Nash equilibrium of a game as in traditional minimization problems. However, in general, gradient descent optimization of smooth games often fail to converge and oscillate around an equilibrium of the game (Daskalakis et al., 2018; Gidel et al., 2019b;a; Letcher et al., 2019). Such non-convergent behavior of game dynamics is mainly due to (non-cooperative) interaction between multiple cost functions, and is considered as a key challenge in the game optimization (Mescheder et al., 2017; 2018; Mazumdar et al., 2019; Hsieh et al., 2020).

2.2 FIRST-ORDER METHODS FOR SMOOTH GAME OPTIMIZATION

We introduce well-known first-order methods for smooth game optimization. To ease the notation, we use $\nabla_{\mathbf{x}}\mathbf{f}(\cdot)$ to denote the concatenated partial derivatives $(\nabla_{\mathbf{x}_1} f_1(\cdot), \ldots, \nabla_{\mathbf{x}_n} f_n(\cdot))$ of a smooth game $\{f_i\}_{i=1}^n$, where $\nabla_{\mathbf{x}_i} f_i(\cdot)$ is a partial derivative of a player i's cost function with respective to its own strategy.

Gradient Descent (GD) minimizes the cost function of each player using the gradient descent. Its simultaneous dynamics $F_{\text{GD}_{\text{Sim}}}$ of a smooth game $\{f_i\}_{i=1}^n$ with a learning rate $\eta > 0$ is given by

$$\mathbf{x}^{(t+1)} = F_{\text{GD}_{\text{Sim}}}(\mathbf{x}^{(t)}) \stackrel{\text{def}}{=} \mathbf{x}^{(t)} - \eta \nabla_{\mathbf{x}} \mathbf{f}(\mathbf{x}^{(t)}). \tag{1}$$

On the other hand, its alternating dynamics $F_{\text{GD}_{\text{Alt}}}$ is described by

$$\mathbf{x}^{(t+1)} = F_{\text{GD}_{\text{Alt}}}(\mathbf{x}^{(t)}) \stackrel{\text{def}}{=} F_1 \circ \ldots \circ F_n(\mathbf{x}^{(t)}), \tag{2}$$

$$F_i(\mathbf{x}) \stackrel{\text{def}}{=} (\ldots, x_{i-1}, x_i - \eta \nabla_{x_i} f_i(\mathbf{x}), x_{i+1}, \ldots). \tag{3}$$

Proximal Point (PP) (Martinet, 1970) computes an update by solving a proximal problem at each iteration. Its simultaneous dynamics $F_{\text{PP}_{\text{Sim}}}$ of a smooth game $\{f_i\}_{i=1}^n$ with a learning rate $\eta > 0$ is

$$\mathbf{x}^{(t+1)} = F_{\text{PP}_{\text{Sim}}}(\mathbf{x}^{(t)}) \stackrel{\text{def}}{=} \mathbf{x}^{(t)} - \eta \nabla_{\mathbf{x}} \mathbf{f}(\mathbf{x}^{(t+1)}). \tag{4}$$

Note that this update rule is implicit in a sense that $\mathbf{x}^{(t+1)}$ appears on both sides of the equation; hence it requires solving the proximal subproblem for $\mathbf{x}^{(t+1)}$ per iteration.

Extra Gradient (EG) (Korpelevich, 1976) computes an update by using an *extrapolated* gradient. Its simultaneous dynamics $F_{\text{EG}_{\text{Sim}}}$ of a smooth game $\{f_i\}_{i=1}^n$ with a learning rate $\eta > 0$ is

$$\mathbf{x}^{(t+1)} = F_{\text{EG}_{\text{Sim}}}(\mathbf{x}^{(t)}) \stackrel{\text{def}}{=} \mathbf{x}^{(t)} - \eta \nabla_{\mathbf{x}} \mathbf{f}(\mathbf{x}^{(t+\frac{1}{2})}), \tag{5}$$

$$\mathbf{x}^{(t+\frac{1}{2})} \stackrel{\text{def}}{=} \mathbf{x}^{(t)} - \eta \nabla_{\mathbf{x}} \mathbf{f}(\mathbf{x}^{(t)}). \tag{6}$$

2.3 Lookahead Optimizer

Lookahead (Zhang et al., 2019) is a recently proposed optimizer that wraps around a base optimizer and takes a *backward* synchronization step for each k *forward* steps. Given a dynamics $F_{\mathcal{A}}$ induced by a base optimization method $\mathcal{A}$, the Lookahead dynamics $G_{\text{LA-}\mathcal{A}}$ with a synchronization period $k \in \mathbb{N}$ and a rate $\alpha \in (0, 1)$ is

$$\mathbf{x}^{(t+1)} = G_{\text{LA-}\mathcal{A}}(\mathbf{x}^{(t)}) \stackrel{\text{def}}{=} (1 - \alpha)\mathbf{x}^{(t)} + \alpha F_{\mathcal{A}}^k(\mathbf{x}^{(t)}). \tag{7}$$

2.4 Related Work

The convergence analysis of first-order smooth game dynamics dates several decades back and have been established in the context of saddle-point problems (Rockafellar, 1976; Korpelevich, 1976; Tseng, 1995), which is a special case of zero-sum games. For example, Rockafellar (1976) showed the linear convergence of PP in the bilinear and strongly-convex-strongly-concave (SCSC) saddle-point problems. Tseng (1995) and Facchinei & Pang (2003) proved the linear convergence of EG in the same problem, and Nemirovski (2004) did in the convex-concave problem over compact sets.

As many learning problems are formulated as games in recent years (Goodfellow et al., 2014; Madry et al., 2018; Silver et al., 2018; Fu et al., 2018; Vinyals et al., 2019), game optimization has regained considerable attentions from the research community. Optimistic gradient descent (OGD) (Popov, 1980), which can be seen as an efficient approximation of EG, was recently rediscovered in the context of GAN training (Daskalakis et al., 2018). Recent work of Liang & Stokes (2019) and Gidel et al. (2019a) proved linear convergence of OGD in bilinear and SCSC games. Mokhtari et al. (2020) established a unifying theoretical framework for analyzing PP, EG and OGD dynamics. Zhang & Yu (2020) presented exact and optimal conditions for PP, EG and OGD dynamics to converge in bilinear games. While there has been a growing interest for incorporating second-order information into game dynamics (Mescheder et al., 2017; Balduzzi et al., 2018; Mazumdar et al., 2019; Schäfer & Anandkumar, 2019; Loizou et al., 2020) to remedy non-convergent behaviors, the first-order optimization still dominates in practice (Brock et al., 2019; Donahue & Simonyan, 2019) due to computational and memory cost of second-order methods.

Lately, Chavdarova et al. (2020) reported that recently developed Lookahead optimizer (Zhang et al., 2019) significantly improves the empirical performance of GANs and reduces the rotational force of bilinear game dynamics. However, this study relied on purely empirical observation and lacked theoretical understanding for Lookahead optimization of smooth games. Although Wang et al. (2020) proved that Lookahead optimizer globally converges to a stationary point in minimization problems, its convergence in smooth games still remain as an open question.

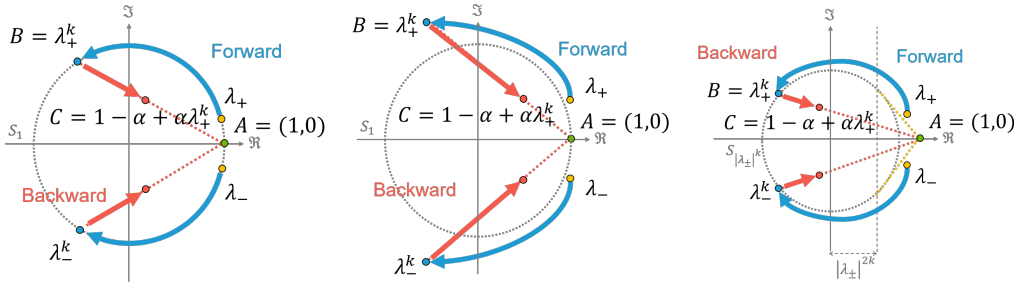

(a) Eigenvalues of GD_{Alt} (b) Eigenvalues of GD_{Sim} (c) Eigenvalues of $\text{PP/EG}_{\text{Sim}}$

Figure 1: The *spectral contraction effect* of Lookahead dynamics in Equation 8. $\lambda_\pm$ are the eigenvalues of each base dynamics, and $1 - \alpha + \alpha\lambda_\pm^k$ are the eigenvalues of the associated Lookahead dynamics. k *forward* steps of a Lookahead procedure first rotate the eigenvalues $\lambda_\pm$ of the dynamics' Jacobian matrix. Then, a synchronization *backward* step pulls them into a circle with a radius smaller than their maximal modulus. This results in a reduced spectral radius of the Jacobian matrix, which improves stability and convergence to an equilibrium.

3 Spectral Contraction Effect of Lookahead in Bilinear Games

In this section, we show that Lookahead can either stabilize or accelerate the convergence of its base dynamics by reducing the spectral radius of its underlying Jacobian matrix. We highlight such *spectral contraction effect* by analyzing convergence of Lookahead dynamics in a simple bilinear game (Section 3.1), and extend the results to general bilinear games (Section 3.2).

3.1 Lookahead Dynamics of a Simple Bilinear Game

We begin with a simple exemplar bilinear game that has a unique Nash equilibrium $(0, 0)$:

$$\min_{x_1 \in \mathbb{R}} \max_{x_2 \in \mathbb{R}} \; x_1 \cdot x_2. \tag{8}$$

This game has been extensively studied as a representative toy example of game optimization by Gidel et al. (2019a) due to its oscillating dynamics. The Following proposition demonstrates stabilization effect of Lookahead on Equation 8.

Proposition 1. *Simultaneous GD dynamics $F_{GD_{Sim}}$ with a learning rate $\eta > 0$ diverges from the Nash equilibrium of Equation 8. However, its Lookahead dynamics $G_{LA\text{-}GD_{Sim}}$ with a synchronization period $k \in \mathbb{N}$ and a rate $\alpha \in (0, 1)$ globally converges to the Nash equilibrium under a proper choice of k and small enough α.*

Proposition 1 shows that a Lookahead optimizer can stabilize divergent dynamics of Equation 8. However, such stabilization effect of Lookahead dynamics raises a natural question: would there be any advantage for using Lookahead when its base dynamics is already stable? Proposition 2 analyzes well-known convergent dynamics of Equation 8, namely PP and EG, and presents an affirmative answer. Specifically, it shows that Lookahead dynamics (i) preserves the stability of its base dynamics, and (ii) can further accelerate their convergence with proper hyperparameter choices.

Proposition 2. *Lookahead dynamics $G_{LA\text{-}PP_{Sim}}$ and $G_{LA\text{-}EG_{Sim}}$ with a learning rate $\eta \in (0, 1)$, a synchronization period $k \in \mathbb{N}$ and a rate $\alpha \in (0, 1)$ globally converges to the Nash equilibrium of Equation 8 under a mild assumption on k. Furthermore, the rate of convergence can be improved upon their base dynamics $F_{PP_{Sim}}$ and $F_{EG_{Sim}}$ with a proper choice of k and a large enough α.*

We provide geometric interpretation of the Lookahead procedure in Figure 1. Intuitively, Lookahead optimizer either stabilizes or accelerates its base dynamics by pulling the eigenvalues of the dynamics' Jacobian matrix into a circle with a small radius. Specifically, k *forward* steps of a Lookahead procedure first rotate the eigenvalues, and a synchronization *backward* step pulls them into a circle with a radius smaller than their maximal modulus. This results in a reduction of the spectral radius of the dynamics' Jacobian matrix, which is known to be crucial for stability (Slotine & Li, 1991). Such *spectral contraction effect* of Lookahead dynamics is captured by the following theorem.

Theorem 3 (Spectral contraction effect of Lookahead)**.** *Let $k \in \mathbb{N}$, $\alpha \in (0,1)$ and define a function $f : \mathbb{M}_{m\times m} \to \mathbb{M}_{m\times m}$ by $f(\boldsymbol{X}) = (1-\alpha)\boldsymbol{I} + \alpha \boldsymbol{X}^k$. Then the following statements hold:*

- *For $\rho(\boldsymbol{X}) = 1$, $\rho(f(\boldsymbol{X})) < 1$ if ${\lambda_{max}}^k \neq 1$, $\forall \lambda_{max} \in eig_{max}(\boldsymbol{X})$.*
- *For $\rho(\boldsymbol{X}) > 1$, $\rho(f(\boldsymbol{X})) < 1$ if $\Re(\lambda_i^k) < 1$, $\alpha < \frac{2\cos(\pi-\theta_i)}{|\lambda_i^k - 1|}$, $\forall \lambda_i \in eig(\boldsymbol{X})$.*
- *For $\rho(\boldsymbol{X}) < 1$, $\rho(f(\boldsymbol{X})) < \rho(\boldsymbol{X})^k$ if $\Re(\lambda_i^k) < \rho(\boldsymbol{X})^{2k}$, $\alpha > 1 - \frac{2\rho(\boldsymbol{X})^k \cos(\pi-\phi_i)}{|\lambda_i^k - 1|}$, $\forall \lambda_i \in eig(\boldsymbol{X})$.*

We define $\theta_i \stackrel{\text{def}}{=} \arg(\lambda_i^k - 1)$ and $\phi_i \stackrel{\text{def}}{=} \arcsin \frac{\sin(\theta_i)}{\rho(\boldsymbol{X})^k}$ for each $\lambda_i \in eig(\boldsymbol{X})$.

Proof. The proof can be found in Appendix E.4. □

Roughly, Theorem 3 suggests that Lookahead can reduce the spectral radius of a matrix by choosing appropriate α and k such that *entire* eigenvalues are rotated to *left enough*. However, such k may not exist, for example, especially when eigenvalues of the matrix are not tightly clustered together. To help understanding when Lookahead can actually reduce the spectral radius, we present Theorem 4 as a sufficient condition for a matrix to admit the existence of k that rotates entire eigenvalues to the left half-plane.

Theorem 4 (Spectrally contractible matrices)**.** *Let $\boldsymbol{X}, \boldsymbol{J} \in \mathbb{M}_{m\times m}$ be matrices such that $\boldsymbol{X} = \boldsymbol{I} - \eta \boldsymbol{J}$ for some $\eta > 0$ and assume that every eigenvalue of $\boldsymbol{J}$ has non-zero imaginary part. Then for any $k \in \mathbb{N}$ with $k \in \left(\frac{\pi}{2\theta_{min}(\boldsymbol{X})}, \frac{3\pi}{2\theta_{max}(\boldsymbol{X})}\right)$, we have $\Re(\lambda_i^k) < 0$ for each $\lambda_i \in eig(\boldsymbol{X})$. Existence of such k is guaranteed for a small enough $\eta > 0$ when $\frac{\Im_{max}(\boldsymbol{J})}{\Im_{min}(\boldsymbol{J})} < 3$.*

Proof. The proof can be found in Appendix E.5. □

Note that the Jacobian matrix of most well-known gradient-based dynamics can be written in the form of $\mathbf{I} - \eta\mathbf{J}$, where $\eta > 0$ is a learning rate and $\mathbf{J}$ is the underlying Jacobian matrix of the game objective. Theorem 4 suggests that for a small enough learning rate, any base dynamics with a imaginary conditioning number less than 3 admits existence of k such that *entire* eigenvalues are rotated to *left enough*. For such k, Lookahead can reduce the spectral radius of a dynamics by choosing proper α, as stated in Theorem 3. To summarize, Theorem 3 and 4 highlight when Lookahead can actually improve game dynamics and show that the imaginary conditioning number of the underlying Jacobian matrix is crucial for determining whether the dynamics is *improvable*.

3.2 Lookahead Dynamics of General Bilinear Games

In this section, we extend the analysis of Lookahead dynamics to a general bilinear game

$$\min_{\mathbf{x}_1 \in \mathbb{R}^m} \max_{\mathbf{x}_2 \in \mathbb{R}^n} \; \mathbf{x}_1^T \mathbf{A} \mathbf{x}_2 - \mathbf{b}_1^T \mathbf{x}_1 - \mathbf{b}_2^T \mathbf{x}_2 \tag{9}$$

for some $\mathbf{A} \in \mathbb{M}_{m\times n}$ and $\mathbf{b}_1 \in \mathbb{R}^m, \mathbf{b}_2 \in \mathbb{R}^n$ such that there exists $\mathbf{x}_1^* \in \mathbb{R}^m, \mathbf{x}_2^* \in \mathbb{R}^n$ with $\mathbf{A}^T \mathbf{x}_1^* = \mathbf{b}_2$ and $\mathbf{A}\mathbf{x}_2^* = \mathbf{b}_1$. The existence of $\mathbf{x}_1^*, \mathbf{x}_2^*$ allows us to rewrite the game as

$$\min_{\mathbf{x}_1 \in \mathbb{R}^n} \max_{\mathbf{x}_2 \in \mathbb{R}^m} \; (\mathbf{x}_1 - \mathbf{x}_1^*)^T \mathbf{U} \begin{bmatrix} \Sigma_r & \mathbf{0} \\ \mathbf{0} & \mathbf{0} \end{bmatrix} \mathbf{V}^T (\mathbf{x}_2 - \mathbf{x}_2^*), \tag{10}$$

where $\mathbf{U}, \Sigma_r, \mathbf{V}$ is a SVD of $\mathbf{A}$ with $r \stackrel{\text{def}}{=} \text{rank}(\mathbf{A})$. We can solve Equation 10 by solving a rather simpler problem

$$\min_{\mathbf{x}_1 \in \mathbb{R}^r} \max_{\mathbf{x}_2 \in \mathbb{R}^r} \; \mathbf{x}_1^T \Sigma_r \mathbf{x}_2, \tag{11}$$

and then changing the coordinates of the obtained solutions by $\mathbf{x}_1 \mapsto \mathbf{U}\left[\mathbf{x}_1; \mathbf{0}_{m-r}\right] + \mathbf{x}_1^*$ and $\mathbf{x}_2 \mapsto \mathbf{V}\left[\mathbf{x}_2; \mathbf{0}_{n-r}\right] + \mathbf{x}_2^*$. This reduction is a well-known technique and has been used by Gidel et al. (2019b;a) and Zhang & Yu (2020) for simplifying the analysis of Equation 9.

We present sufficient conditions on Lookahead hyperparameters under which each of the first-order Lookahead dynamics can be improved upon their base dynamics. The following theorems show that Lookahead can provably stabilize or accelerate the convergence of its base dynamics of bilinear games when the condition number $\frac{\sigma_{max}}{\sigma_{min}}$ of the game matrix $\mathbf{A}$ is less than 3.

Theorem 5 (Convergence of $G_{\text{LA-GD}_{\text{Alt}}}$)**.** *Lookahead dynamics $G_{\text{LA-GD}_{\text{Alt}}}$ with a learning rate $\eta \in \left(0, \frac{2}{\sigma_{max}}\right)$, a synchronization period $k \in \mathbb{N}$ and a rate $\alpha \in (0,1)$ converges to a Nash equilibrium of Equation 9 when k is such that $k \arccos(1 - \frac{\eta^2\sigma_i^2}{2}) \bmod \pi \neq 0$ for any σ_i.*

Proof. The proof can be found in Appendix E.6. □

Theorem 6 (Convergence of $G_{\text{LA-GD}_{\text{Sim}}}$)**.** *Lookahead dynamics $G_{\text{LA-GD}_{\text{Sim}}}$ with a small enough learning rate $\eta > 0$, a synchronization period $k \in \mathbb{N}$ with $k \in \left(\frac{\pi}{2\arctan \eta\sigma_{min}}, \frac{3\pi}{2\arctan \eta\sigma_{max}}\right)$ and a small enough rate $\alpha \in (0,1)$ converges to a Nash equilibrium of Equation 9 when $\frac{\sigma_{max}}{\sigma_{min}} < 3$ and k is such that $k \arctan \eta\sigma_i \bmod \pi \neq 0$ for any σ_i.*

Proof. The proof can be found in Appendix E.7. □

Theorem 7 (Acceleration of $G_{\text{LA-PP}_{\text{Sim}}}$)**.** *Lookahead dynamics $G_{\text{LA-PP}_{\text{Sim}}}$ with a learning rate $\eta > 0$, a synchronization period $k \in \mathbb{N}$ and a rate $\alpha \in (0,1)$ converges to a Nash equilibrium of Equation 9 when k is such that $k \arctan \eta\sigma_i \bmod \pi \neq 0$ for any σ_i. Furthermore, the rate of convergence is accelerated upon its base dynamics $F_{\text{PP}_{\text{Sim}}}$ for a small enough η, $k \in \left(\frac{\pi}{2\arctan \eta\sigma_{min}}, \frac{3\pi}{2\arctan \eta\sigma_{max}}\right)$ and some large enough α when $\frac{\sigma_{max}}{\sigma_{min}} < 3$.*

Proof. The proof can be found in Appendix E.8. □

Theorem 8 (Acceleration of $G_{\text{LA-EG}_{\text{Sim}}}$)**.** *Lookahead dynamics $G_{\text{LA-EG}_{\text{Sim}}}$ with a learning rate $\eta \in \left(0, \frac{1}{\sigma_{max}}\right)$, a synchronization period $k \in \mathbb{N}$ and a rate $\alpha \in (0,1)$ converges to a Nash equilibrium of Equation 9 when k is such that $k \arctan \frac{\eta\sigma_i}{1-\eta\sigma_i} \bmod \pi \neq 0$ for any σ_i. Furthermore, the rate of convergence is accelerated upon its base dynamics $F_{\text{EG}_{\text{Sim}}}$ for a small enough η, $k \in \left(\frac{\pi}{2\arctan \frac{\eta\sigma_{min}}{1-\eta\sigma_{min}}}, \frac{3\pi}{2\arctan \frac{\eta\sigma_{max}}{1-\eta\sigma_{max}}}\right)$ and some large enough α when $\frac{\sigma_{max}}{\sigma_{min}} < 3$.*

Proof. The proof can be found in Appendix E.9. □

4 Limit Points of Lookahead Dynamics

In this section, we characterize the limit points of Lookahead dynamics and reveal the connections between their stability and the hyperparameters of Lookahead. We start by defining a few stability concepts which are standard in the dynamical system theory (Slotine & Li, 1991).

Definition 3 (Lyapunov stability)**.** *Let F be a smooth vector field on $\mathbb{R}^n$. Then $\boldsymbol{x} \in \mathbb{R}^n$ is Lyapunov stable in F if for any $\epsilon > 0$, there exists $\delta > 0$ such that for any $\boldsymbol{y} \in \mathbb{R}^n$, $\|\boldsymbol{x} - \boldsymbol{y}\| < \delta$ implies $\|F^t(\boldsymbol{x}) - F^t(\boldsymbol{y})\| < \epsilon$ for all $t \in \mathbb{N}$.*

Definition 4 (Asymptotic stability)**.** *A Lyapunov stable equilibrium $\boldsymbol{x}^* \in \mathbb{R}^n$ of a smooth vector field F is said to be asymptotically stable if there exists $\delta > 0$ such that $\|\boldsymbol{x} - \boldsymbol{x}^*\| < \delta$ implies $\lim_{t\to\infty} \|F^t(\boldsymbol{x}) - \boldsymbol{x}^*\| = 0$. Such $\boldsymbol{x}^*$ is said to be locally asymptotically stable if $\delta < \infty$.*

Now we show that Lookahead preserves locally asymptotically stable equilibria of its base dynamics, and it can either stabilize or accelerate the local convergence to an equilibrium. Furthermore, we directly follow the approach of Daskalakis & Panageas (2018) and derive a connection between the Lipschitz constant of a base dynamics and the long-term behavior of its Lookahead dynamics.

Theorem 9 ($\text{LASE}_{\mathcal{A}} \subseteq \text{LASE}_{\text{LA-}\mathcal{A}}$)**.** *Let $\boldsymbol{x}^*$ be a locally asymptotically stable equilibrium (LASE) of a dynamics F. Then, $\boldsymbol{x}^*$ is also a LASE of its Lookahead dynamics G with a synchronization period $k \in \mathbb{N}$ and a rate $\alpha \in (0,1)$ if $\lambda_i^k \neq 1$ for each $\lambda_i \in eig(\nabla_{\boldsymbol{x}} F(\boldsymbol{x}^*))$.*

Proof. The proof can be found in Appendix E.10. □

Theorem 10 (One-point local stabilization)**.** *Let $\boldsymbol{x}^* \in \mathbb{R}^n$ be an equilibrium of a dynamics F with $\rho(\nabla_{\boldsymbol{x}} F(\boldsymbol{x}^*)) > 1$. Assume $\boldsymbol{J} \in \mathbb{M}_{n\times n}$ is such that $\nabla_{\boldsymbol{x}} F(\boldsymbol{x}^*) = \boldsymbol{I} - \eta \boldsymbol{J}$ for some $\eta > 0$ and every eigenvalue of $\boldsymbol{J}$ has non-zero imaginary part. Then for a small enough η, $\boldsymbol{x}^*$ is a LASE of its Lookahead dynamics G with a synchronization period $k \in \left(\frac{\pi}{2\theta_{min}(\nabla_{\boldsymbol{x}} F(\boldsymbol{x}^*))}, \frac{3\pi}{2\theta_{max}(\nabla_{\boldsymbol{x}} F(\boldsymbol{x}^*))}\right)$ and a small enough rate $\alpha \in (0, 1)$ when $\frac{\Im_{max}(\boldsymbol{J})}{\Im_{min}(\boldsymbol{J})} < 3$.*

Proof. The proof can be found in Appendix E.11. □

Theorem 11 (One-point local acceleration)**.** *Let $\boldsymbol{x}^* \in \mathbb{R}^n$ be an equilibrium of a dynamics F with $\rho(\nabla_{\boldsymbol{x}} F(\boldsymbol{x}^*)) < 1$. Assume $\boldsymbol{J} \in \mathbb{M}_{n\times n}$ is such that $\nabla_{\boldsymbol{x}} F(\boldsymbol{x}^*) = \boldsymbol{I} - \eta \boldsymbol{J}$ for some $\eta > 0$ and every eigenvalue of $\boldsymbol{J}$ has non-zero imaginary part. Then for a small enough η, the rate of local convergence to $\boldsymbol{x}^*$ in a Lookahead dynamics G with a synchronization period $k \in \left(\frac{\pi}{2\theta_{min}(\nabla_{\boldsymbol{x}} F(\boldsymbol{x}^*))}, \frac{3\pi}{2\theta_{max}(\nabla_{\boldsymbol{x}} F(\boldsymbol{x}^*))}\right)$ and a large enough rate $\alpha \in (0, 1)$ is accelerated upon the rate of dynamics F when $\frac{\Im_{max}(\boldsymbol{J})}{\Im_{min}(\boldsymbol{J})} < 3$.*

Proof. The proof can be found in Appendix E.12. □

Theorem 12 (Avoids unstable points)**.** *Let F be a L-Lipschitz smooth dynamics for some $L > 0$ and let G be its Lookahead dynamics with a synchronization period $k \in \mathbb{N}$ and a rate $\alpha \in \left(0, \frac{1}{1+L^k}\right)$. Then the iterates of G almost surely avoids its equilibrium $\boldsymbol{x}^*$ with $\rho(\nabla_{\boldsymbol{x}} G(\boldsymbol{x}^*)) > 1$ when $\rho(\nabla_{\boldsymbol{x}} G(\boldsymbol{x}_0)) \neq 1$ holds for any equilibrium $\boldsymbol{x}_0$ of G.*

Proof. The proof can be found in Appendix E.13. □

To summarize, Theorem 9 shows that any locally asymptotically stable equilibrium (LASE) of a base dynamics is also a LASE of its Lookahead dynamics. Theorem 10–11 suggest that Lookahead dynamics can either stabilize or accelerate the local convergence to an equilibrium of a dynamics if when its Jacobian imaginary conditioning is less than 3. Lastly, Theorem 12 indicates that we need to choose a small α to guarantee the avoidance of unstable points when its base dynamics is quite turbulent, *i.e.*, has large Lipschitz constant.

5 EXPERIMENTS

Bilinear game. We test our theoretical predictions in Section 3.2 (Theorem 5–8) on a bilinear game

$$\min_{\mathbf{x}_1 \in \mathbb{R}^n} \max_{\mathbf{x}_2 \in \mathbb{R}^n} \mathbf{x}_1^T \mathbf{A} \mathbf{x}_2 \tag{12}$$

with $\mathbf{A} \stackrel{\text{def}}{=} \mathbf{I}_n + \epsilon \cdot \mathbf{E}_n$, where each element of $\mathbf{E}_n \in \mathbb{M}_{n\times n}$ is sampled from $\mathcal{N}(0, 1)$. We report our results using $n = 10$ and $\epsilon = 0.05$, which gives a sample of $\mathbf{A}$ with $\sigma_{max} = 1.195$ and $\sigma_{min} = 0.852$, hence $\frac{\sigma_{max}}{\sigma_{min}} = 1.401 < 3$. For a fixed $\eta = 0.1$, we use Theorem 5–8 to derive a range of k and an approximate scale of α that guarantee stabilization and acceleration of convergence to a Nash equilibrium (NE) of Equation 12. We provide the derivations of theoretically recommended values and actual configurations used for the experiment in Appendix D. Figure 2 (a) shows that the hyperparameters predicted by our theorems, denoted by LA-GD$_{\text{Alt/Sim}}{}^{+}$ and LA-EG$_{\text{Sim}}{}^{+}$, actually stabilize and accelerates the convergence to a NE. We also test the hyperparameters that are chosen against our theorems and denote as LA-GD$_{\text{Alt/Sim}}{}^{-}$ and LA-EG$_{\text{Sim}}{}^{-}$. Specifically, we choose a k smaller than the lower bound predicted by our theorems and use large α for unstable base dynamics and small α for stable base dynamics. The result in Figure 2 (a) suggests that Lookahead can fail to stabilize, or even worse, slow down the convergence when hyperparameters are configured badly.

Nonlinear game with a protected unstable equilibrium. We verify our theoretical predictions in Section 4 (Theorem 10 and 11) on the non-linear game proposed by Hsieh et al. (2020):

$$\min_{x_1 \in \mathbb{R}} \max_{x_2 \in \mathbb{R}} \; x_1 \cdot x_2 + \epsilon \phi(x_2), \tag{13}$$

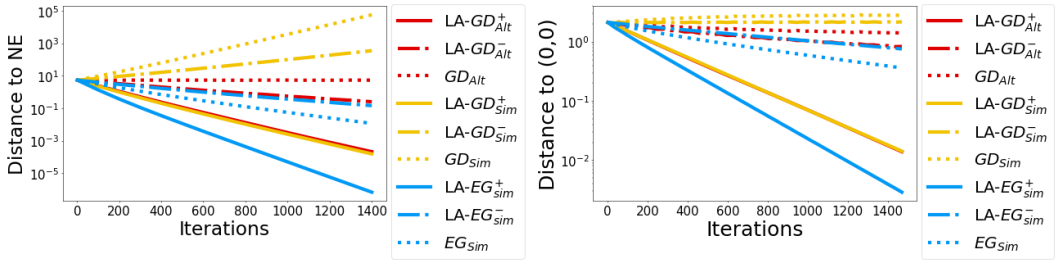

(a) Convergence to NE of the bilinear game. (b) Convergence to equilibrium in the nonlinear game.

Figure 2: Optimization progress of multiple first-order methods with hyperparameters predicted by our theorems $(+)$ and chosen against our theorems $(-)$ in the bilinear and nonlinear games.

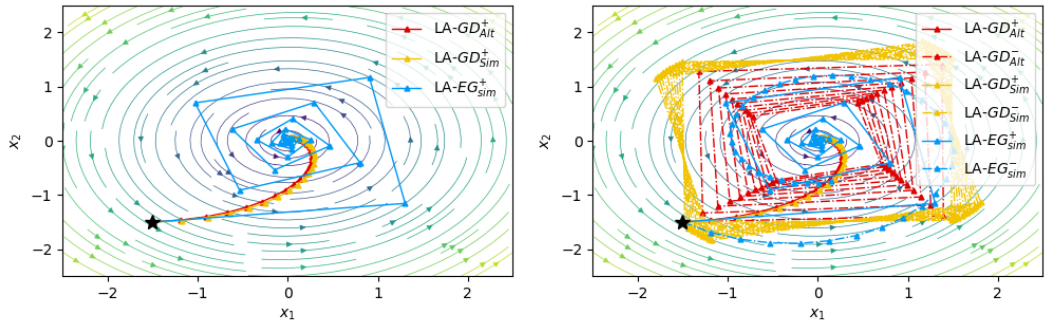

(a) Hyperparameters predicted by Theorem 10,11 (b) Hyperparameters chosen against Theorem 10,11

Figure 3: Visualized trajectory of each dynamics to the equilibrium $(0, 0)$ of the nonlinear game.

where $\phi(x) \stackrel{\text{def}}{=} \frac{1}{2}x^2 - \frac{1}{4}x^4$ with $\epsilon > 0$. This game has an unstable critical point $(0, 0)$ surrounded by an attractive internally chain-transitive (ICT) set, which may contain arbitrarily long trajectories. Hsieh et al. (2020) demonstrate that most first-order methods fail to converge in this game due to the instability of the equilibrium and the existence of the ICT set. For a fixed $\epsilon = 0.01$ and $\eta = 0.05$, we use Theorem 10 and 11 to derive a range of k and an approximate scale of α that guarantee local stabilization and acceleration to the equilibrium of Equation 13. We provide the detailed derivations of the theoretically recommended values and the configurations in Appendix D. Figure 2 (b) and Figure 3 (a) shows that the hyperparameters predicted by our theorems, denoted by LA-GD$_{\text{Alt/Sim}}{}^+$ and LA-EG$_{\text{Sim}}{}^+$, actually stabilize and accelerates the convergence to the equilibrium. In contrast, hyperparameters chosen against our theorems, denoted by LA-GD$_{\text{Alt/Sim}}{}^-$ and LA-EG$_{\text{Sim}}{}^-$ in Figure 2 (b) and Figure 3 (b), neither success to stabilize nor accelerate the convergence to the equilibrium.

6 Conclusion

In this work, we derived the theoretic results for convergence guarantee and acceleration of Lookahead dynamics in smooth games for the first time. Specifically, we derived sufficient conditions for hyperparameters of Lookahead optimizer under which the convergence of bilinear games is either stabilized or accelerated. Furthermore, we proved that the Lookahead optimizer preserves locally asymptotically stable equilibria of smooth games. Finally, we showed that Lookahead can either stabilize or accelerate the local convergence to a given equilibrium under proper assumptions.

Our results point to several future research directions. Theorem 4 suggests that the imaginary conditioning of the underlying Jacobian matrix is crucial for the performance gain in Lookahead. Therefore, developing an optimization method that exhibits a small imaginary conditioning could improve the convergence of its Lookahead dynamics. Another interesting application of our theoretic results would be designing an adaptive mechanism for the Lookahead hyperparameters by applying our theorems on local bilinear approximation (Schäfer & Anandkumar, 2019) of the game for each step.

REFERENCES

D. Balduzzi, Sébastien Racanière, J. Martens, Jakob N. Foerster, K. Tuyls, and T. Graepel. The Mechanics of n-Player Differentiable Games. In *ICML*, 2018.

Trapit Bansal, Jakub W. Pachocki, S. Sidor, Ilya Sutskever, and Igor Mordatch. Emergent Complexity via Multi-Agent Competition. In *ICLR*, 2018.

D.P. Bertsekas. *Nonlinear Programming*. Athena Scientific, 1999.

A. Brock, J. Donahue, and K. Simonyan. Large Scale GAN Training for High Fidelity Natural Image Synthesis. In *ICLR*, 2019.

Tatjana Chavdarova, Matteo Pagliardini, M. Jaggi, and Franois Fleuret. Taming GANs with Lookahead. *ArXiv*, abs/2006.14567, 2020.

X. Chen, X. Deng, and S. Teng. Settling the Complexity of Computing Two-player Nash Equilibria. *J. ACM*, 56:14:1–14:57, 2009.

C. Daskalakis and Ioannis Panageas. The Limit Points of (Optimistic) Gradient Descent in Min-Max Optimization. In *NeurIPS*, 2018.

C. Daskalakis, P. Goldberg, and C. Papadimitriou. The Complexity of Computing a Nash Equilibrium. *Electron. Colloquium Comput. Complex.*, 2006.

C. Daskalakis, Andrew Ilyas, Vasilis Syrgkanis, and Haoyang Zeng. Training GANs with Optimism. In *ICLR*, 2018.

J. Donahue and K. Simonyan. Large Scale Adversarial Representation Learning. In *NeurIPS*, 2019.

F. Facchinei and J. Pang. *Finite-Dimensional Variational Inequalities and Complementarity Problems*. Springer, 2003.

Justin Fu, Katie Luo, and S. Levine. Learning Robust Rewards with Adversarial Inverse Reinforcement Learning. In *ICLR*, 2018.

Gauthier Gidel, Hugo Berard, Pascal Vincent, and S. Lacoste-Julien. A Variational Inequality Perspective on Generative Adversarial Nets. In *ICLR*, 2019a.

Gauthier Gidel, Reyhane Askari Hemmat, M. Pezeshki, Gabriel Huang, Rémi Le Priol, S. Lacoste-Julien, and Ioannis Mitliagkas. Negative Momentum for Improved Game Dynamics. In *AISTAT*, 2019b.

Ian J. Goodfellow. NIPS 2016 Tutorial: Generative Adversarial Networks. *ArXiv*, abs/1701.00160, 2017.

Ian J. Goodfellow, Jean Pouget-Abadie, M. Mirza, Bing Xu, David Warde-Farley, Sherjil Ozair, Aaron C. Courville, and Yoshua Bengio. Generative Adversarial Nets. In *NIPS*, 2014.

Ian J. Goodfellow, Jonathon Shlens, and Christian Szegedy. Explaining and Harnessing Adversarial Examples. *CoRR*, abs/1412.6572, 2015.

Ya-Ping Hsieh, Panayotis Mertikopoulos, and Volkan Cevher. The Limits of Min-Max Optimization Algorithms: Convergence to Spurious Non-critical Sets. *ArXiv*, abs/2006.09065, 2020.

Tero Karras, S. Laine, and Timo Aila. A Style-Based Generator Architecture for Generative Adversarial Networks. In *CVPR*, 2019.

Diederik P. Kingma and Jimmy Ba. Adam: A Method for Stochastic Optimization. In *ICLR*, 2015.

G. M. Korpelevich. The Extragradient Method for Finding Saddle Points and Other Problems. *Ekonomika i Matematicheskie Metody*, 12:747–756, 1976.

Marc Lanctot, V. Zambaldi, A. Gruslys, A. Lazaridou, K. Tuyls, Julien Pérolat, D. Silver, and T. Graepel. A Unified Game-Theoretic Approach to Multiagent Reinforcement Learning. In *NeurIPS*, 2017.

J. Lee, Ioannis Panageas, G. Piliouras, Max Simchowitz, Michael I. Jordan, and B. Recht. First-order methods almost always avoid saddle points. In *NeurIPS*, 2019.

Alistair Letcher, D. Balduzzi, Sébastien Racanière, J. Martens, Jakob N. Foerster, K. Tuyls, and T. Graepel. Differentiable Game Mechanics. *JMLR*, 20:1–40, 2019.

Tengyuan Liang and J. Stokes. Interaction Matters: A Note on Non-asymptotic Local Convergence of Generative Adversarial Networks. In *AISTATS*, 2019.

N. Loizou, Hugo Berard, Alexia Jolicoeur-Martineau, Pascal Vincent, S. Lacoste-Julien, and Ioannis Mitliagkas. Stochastic Hamiltonian Gradient Methods for Smooth Games. In *ICML*, 2020.

A. Madry, Aleksandar Makelov, L. Schmidt, D. Tsipras, and Adrian Vladu. Towards Deep Learning Models Resistant to Adversarial Attacks. In *ICLR*, 2018.

B. Martinet. Brève Communication. Régularisation d'inéquations Variationnelles par Approximations Successives. *ESAIM: Mathematical Modelling and Numerical Analysis - Modélisation Mathématique et Analyse Numérique*, 4(R3):154–158, 1970.

Eric V. Mazumdar, Michael I. Jordan, and S. Sastry. On Finding Local Nash Equilibria (and Only Local Nash Equilibria) in Zero-Sum Games. *ArXiv*, abs/1901.00838, 2019.

P. Mertikopoulos, C. Papadimitriou, and G. Piliouras. Cycles in Adversarial Regularized Learning. In *SODA*, 2018.

P. Mertikopoulos, Houssam Zenati, Bruno Lecouat, Chuan-Sheng Foo, V. Chandrasekhar, and G. Piliouras. Mirror descent in saddle-point problems: Going the extra (gradient) mile. *ArXiv*, abs/1807.02629, 2019.

Lars M. Mescheder, Sebastian Nowozin, and Andreas Geiger. The Numerics of GANs. In *NIPS*, 2017.

Lars M. Mescheder, Andreas Geiger, and Sebastian Nowozin. Which Training Methods for GANs do actually Converge? In *ICML*, 2018.

Aryan Mokhtari, A. Ozdaglar, and Sarath Pattathil. A Unified Analysis of Extra-gradient and Optimistic Gradient Methods for Saddle Point Problems: Proximal Point Approach. In *AISTATS*, 2020.

Cristinel Mortici and Hary M Srivastava. Estimates for the Arctangent Function Related to Shafer's Inequality. *Colloq. Math*, 136(2):263–270, 2014.

J. Nash. Non-Cooperative Games. *Annals of Mathematics*, 54:286, 1951.

A. Nemirovski. Prox-Method with Rate of Convergence O(1/t) for Variational Inequalities with Lipschitz Continuous Monotone Operators and Smooth Convex-Concave Saddle Point Problems. *SIAM J. Optim.*, 15:229–251, 2004.

L. Popov. A modification of the arrow-hurwicz method for search of saddle points. *Mathematical notes of the Academy of Sciences of the USSR*, 28:845–848, 1980.

R. T. Rockafellar. Monotone Operators and the Proximal Point Algorithm. *Siam Journal on Control and Optimization*, 14:877–898, 1976.

Florian Schäfer and Anima Anandkumar. Competitive Gradient Descent. In *NeurIPS*, 2019.

D. Silver, T. Hubert, Julian Schrittwieser, Ioannis Antonoglou, Matthew Lai, A. Guez, Marc Lanctot, L. Sifre, D. Kumaran, T. Graepel, T. Lillicrap, K. Simonyan, and Demis Hassabis. A General Reinforcement Learning Algorithm That Masters Chess, Shogi, and Go Through Self-play. *Science*, 362:1140 – 1144, 2018.

J. Slotine and W. Li. *Applied Nonlinear Control*. Pearson, 1991.

P. Tseng. On Linear Convergence of Iterative Methods for the Variational Inequality Problem. *Journal of Computational and Applied Mathematics*, 60:237–252, 1995.

Oriol Vinyals, I. Babuschkin, W. Czarnecki, Michaël Mathieu, A. Dudzik, J. Chung, D. Choi, R. Powell, Timo Ewalds, P. Georgiev, Junhyuk Oh, Dan Horgan, Manuel Kroiss, Ivo Danihelka, Aja Huang, L. Sifre, Trevor Cai, John P. Agapiou, Max Jaderberg, A. S. Vezhnevets, Rémi Leblond, Tobias Pohlen, Valentin Dalibard, D. Budden, Yury Sulsky, James Molloy, T. L. Paine, Caglar Gulcehre, Ziyu Wang, T. Pfaff, Yuhuai Wu, Roman Ring, Dani Yogatama, Dario Wünsch, Katrina McKinney, O. Smith, T. Schaul, T. Lillicrap, K. Kavukcuoglu, Demis Hassabis, Chris Apps, and D. Silver. Grandmaster Level in StarCraft II using Multi-agent Reinforcement Learning. *Nature*, pp. 1–5, 2019.

Jianyu Wang, Vinayak Tantia, Nicolas Ballas, and Michael Rabbat. Lookahead Converges to Stationary Points of Smooth Non-convex Functions. In *ICASSP*, 2020.

Yasin Yazici, C. S. Foo, S. Winkler, Kim-Hui Yap, G. Piliouras, and V. Chandrasekhar. The Unusual Effectiveness of Averaging in GAN Training. In *ICLR*, 2019.

Guojun Zhang and Y. Yu. Convergence of Gradient Methods on Bilinear Zero-Sum Games. In *ICLR*, 2020.

M. Zhang, J. Lucas, Geoffrey E. Hinton, and Jimmy Ba. Lookahead Optimizer: k Steps Forward, 1 Step Back. In *NeurIPS*, 2019.

A NOTATION

Table A.1: List of mathematical notations used in the paper.

Symbol	Definition
$\|\cdot\|$	L^2 norm
x_i	i-th element of a vector $\mathbf{x} = (x_1, \dots, x_n)$
$\mathbf{x}_i$	i-th vector of a concatenated vectors $\mathbf{x} = (\mathbf{x}_1, \dots, \mathbf{x}_n)$
$\mathbf{x}_{-i}$	$(\mathbf{x}_1, \dots, \mathbf{x}_{i-1}, \mathbf{x}_{i+1}, \dots, \mathbf{x}_n)$
$\nabla_x f(x')$	Derivative of a function f evaluated at x'
S_r	The zero-centered circle of radius $r > 0$ in $\mathbb{C}$
$\Re(z)$	Real part of $z \in \mathbb{C}$
$\Im(z)$	Imaginary part of $z \in \mathbb{C}$
$\arg(z)$	The angle between $z \in \mathbb{C}$ and real axis of the complex plane
$\sigma(\mathbf{A})$	The set of singular values of $\mathbf{A} \in \mathbb{M}_{m\times n}$
$\rho(\mathbf{A})$	The spectral radius of $\mathbf{A} \in \mathbb{M}_{m\times m}$
$\text{eig}(\mathbf{A})$	The set of eigenvalues of $\mathbf{A} \in \mathbb{M}_{m\times m}$
$\text{eig}_{\text{max}}(\mathbf{A})$	The set of eigenvalues of $\mathbf{A}$ with the largest modulus
$\Re(\mathbf{A})$	$\{\Re(\lambda_i) \| \lambda_i \in \text{eig}(\mathbf{A})\}$
$\Re_{min}(\mathbf{A})$	$\min \Re(\mathbf{A})$
$\Re_{max}(\mathbf{A})$	$\max \Re(\mathbf{A})$
$\Im(\mathbf{A})$	$\{\Im(\lambda_i) \| \lambda_i \in \text{eig}(\mathbf{A})\}$
$\Im_{\geq 0}(\mathbf{A})$	$\{\Im_i \in \Im(\mathbf{A}) \| \Im_i \geq 0\}$
$\Im_{min}(\mathbf{A})$	$\min \Im_{\geq 0}(\mathbf{A})$
$\Im_{max}(\mathbf{A})$	$\max \Im_{\geq 0}(\mathbf{A})$
$\theta(\mathbf{A})$	$\{\arg(\lambda_i) \| \lambda_i \in \text{eig}(\mathbf{A})\}$
$\theta_{\geq 0}(\mathbf{A})$	$\{\theta_i \| \theta_i \in \theta(\mathbf{A}), \theta_i \geq 0\}$
$\theta_{min}(\mathbf{A})$	$\min \theta_{\geq 0}(\mathbf{A})$
$\theta_{max}(\mathbf{A})$	$\max \theta_{\geq 0}(\mathbf{A})$

B USEFUL FACTS

B.1 STANDARD RESULTS ON CONVERGENCE

Proposition 13 (Bertsekas (1999))**.** *Let $F : \mathbb{R}^m \to \mathbb{R}^m$ be continuously differentiable, and let $\boldsymbol{x}^* \in \mathbb{R}^m$ be such that $F(\boldsymbol{x}^*) = \boldsymbol{x}^*$. Assume that $\rho(\nabla_{\boldsymbol{x}} F(\boldsymbol{x}^*)) < 1$. Then, there is an open neighborhood $U_{\boldsymbol{x}^*}$ of $\boldsymbol{x}^*$ such that for any $\boldsymbol{x} \in U_{\boldsymbol{x}^*}$, $\|F^t(\boldsymbol{x}) - \boldsymbol{x}^*\|_2 \in \mathcal{O}(\rho(\nabla_{\boldsymbol{x}} F(\boldsymbol{x}^*))^t)$ for $t \to \infty$.*

Lemma 14 (Gidel et al. (2019b))**.** *Let $\boldsymbol{M} \in \mathbb{R}^{m\times m}$ and $\boldsymbol{u}^{(t)}$ be a sequence of iterates such that, $\boldsymbol{u}^{(t+1)} = \boldsymbol{M}\boldsymbol{u}^{(t)}$, then we have three cases of interest for the spectral radius $\rho(\boldsymbol{M})$:*

- *If $\rho(\boldsymbol{M}) < 1$ and $\boldsymbol{M}$ is diagonalizable, then $\left\|\boldsymbol{u}^{(t)}\right\|_2 \in \mathcal{O}(\rho(\boldsymbol{M})^t \left\|\boldsymbol{u}^{(0)}\right\|_2)$.*
- *If $\rho(\boldsymbol{M}) > 1$, then there exists $\boldsymbol{u}^{(0)}$ such that $\left\|\boldsymbol{u}^{(t)}\right\|_2 \in \Omega(\rho(\boldsymbol{M})^t \left\|\boldsymbol{u}^{(0)}\right\|_2)$.*
- *If $|\lambda_i| = 1, \forall \lambda_i \in eig(\boldsymbol{M})$, and $\boldsymbol{M}$ is diagonalizable, then $\left\|\boldsymbol{u}^{(t)}\right\|_2 \in \Theta(\left\|\boldsymbol{u}^{(0)}\right\|_2)$.*

B.2 CHARACTERISTIC EQUATIONS OF FIRST-ORDER DYNAMICS IN BILINEAR GAMES

Latest work of Zhang & Yu (2020) provides the exact and optimal conditions for popular first-order methods to converge in zero-sum bilinear games, if possible. Besides from the exact conditions and the choice of optimal hyperparameters, they also derive the characteristic equation of each first-order dynamics in the zero-sum bilinear games. Since our proofs of theorems in Section 3.2 heavily rely on these characteristic equations, we restate somewhat simplified version of the equations for

Equation 9 using our notations.

$$\text{GD}_{\text{Alt}}: \ (\lambda_i - 1)^2 + \eta^2\sigma_i^2\lambda_i = 0. \tag{14}$$

$$\text{GD}_{\text{Sim}}: \ (\lambda_i - 1)^2 + \eta^2\sigma_i^2 = 0. \tag{15}$$

$$\text{PP}_{\text{Sim}}: \ (1/\lambda_i - 1)^2 + \eta^2\sigma_i^2 = 0. \tag{16}$$

$$\text{EG}_{\text{Alt}}: \ (\lambda_i - 1)^2 + (\eta^2 + 2\eta)\sigma_i^2(\lambda_i - 1) + (\eta^2\sigma_i^2 + \eta^2\sigma_i^4) = 0. \tag{17}$$

$$\text{EG}_{\text{Sim}}: \ (\lambda_i - 1)^2 + 2\eta\sigma_i^2(\lambda_i - 1) + \eta^2\sigma_i^2 + \eta^2\sigma_i^4 = 0. \tag{18}$$

We denote the singular values of matrix $\mathbf{A}$ in Equation 9 by σ_i. The eigenvalues of each dynamics' Jacobian matrix are denoted by λ_i. Note that Zhang & Yu (2020) also derive characteristic equations of memory-augmented first-order methods, such as OGD (Popov, 1980) and the momentum method, which we do not cover in this paper.

C Omitted Results

Proposition 15. *Alternating GD dynamics $F_{GD_{Alt}}$ with a learning rate $\eta \in (0, 2)$ fails to converge and oscillates around the Nash equilibrium of the game in Equation 8. However, its Lookahead dynamics $G_{LA\text{-}GD_{Alt}}$ with a synchronization period $k \in \mathbb{N}$ and a rate $\alpha \in (0, 1)$ globally converges to the Nash equilibrium under a mild assumption on k.*

Proof. One can easily check from Equation 2 that the dynamics $F_{\text{GD}_{\text{Alt}}}$ can be written as

$$F_{\text{GD}_{\text{Alt}}}(x_1^{(t)}, x_2^{(t)}) = \begin{bmatrix} 1 & -\eta \\ \eta & 1 - \eta^2 \end{bmatrix} \begin{bmatrix} x_1^{(t)} \\ x_2^{(t)} \end{bmatrix}. \tag{19}$$

Defining $\mathbf{M} \stackrel{\text{def}}{=} \begin{bmatrix} 1 & -\eta \\ \eta & 1 - \eta^2 \end{bmatrix}$, the Lookahead dynamics $G_{\text{LA-GD}_{\text{Alt}}}$ can be written as

$$G_{\text{LA-GD}_{\text{Alt}}}(x_1^{(t)}, x_2^{(t)}) = ((1 - \alpha)\mathbf{I} + \alpha\mathbf{M}^k) \begin{bmatrix} x_1^{(t)} \\ x_2^{(t)} \end{bmatrix}. \tag{20}$$

It follows that the eigenvalues of $\nabla_{\mathbf{x}} G_{\text{LA-GD}_{\text{Alt}}}$ can be written as $1 - \alpha + \alpha\lambda_\pm^k$ with $\lambda_\pm \stackrel{\text{def}}{=} 1 - \eta\frac{\eta \pm i\sqrt{4-\eta^2}}{2} \in \text{eig}(\mathbf{M})$ for any $\eta \in (0, 2)$. Let us choose k such that $\lambda_\pm^k \notin \{1, -1\}$. Then, $(1 - \alpha)\mathbf{I} + \alpha\mathbf{M}^k$ is diagonalizable as it admits complex conjugate eigenvalues $1 - \alpha + \alpha\lambda_\pm^k$. Furthermore, we know that $1 - \alpha + \alpha\lambda_\pm^k$ is an interpolation between two distinct points on S_1 since $|\lambda_\pm| = 1$ and $\lambda_\pm^k \neq 1$, implying $|1 - \alpha + \alpha\lambda_\pm^k| < 1$. Therefore we conclude from Lemma 14 that the iterates of $G_{\text{LA-GD}_{\text{Alt}}}$ converge to the Nash equilibrium $(0, 0)$ of the game with convergence rate $\mathcal{O}(|1 - \alpha + \alpha\lambda_\pm^k|^{t/k})$, assuming the amortization of its computation over k forward steps. The proof for oscillation of $F_{\text{GD}_{\text{Alt}}}$ follows from Lemma 14 and can be found in Gidel et al. (2019a). □

Proposition 16 (Equilibrium of Lookahead dynamics)**.** *Let F be a dynamics and G be its associated Lookahead dynamics with a synchronization period $k \in \mathbb{N}$. Then any equilibrium of F is an equilibrium of G and any equilibrium of G is a periodic point of F.*

Proof. Let $k \in \mathbb{N}$ and $\alpha \in (0, 1)$ be the synchronization period and synchronization rate of G, respectively. It is trivial to see that $G(\mathbf{x}^*) = ((1 - \alpha)id + \alpha F^k)(\mathbf{x}^*) = (1 - \alpha)\mathbf{x}^* + \alpha\mathbf{x}^* = \mathbf{x}^*$ if $F(\mathbf{x}^*) = \mathbf{x}^*$. Conversely, one can easily check that $G(\mathbf{x}^*) = (1 - \alpha)\mathbf{x}^* + \alpha F^k(\mathbf{x}^*) = \mathbf{x}^*$ implies $F^k(\mathbf{x}^*) = \mathbf{x}^*$. □

D EXPERIMENTAL DETAILS

We report the actual hyperparameters used for the experiments of Section 5 in TableD.2 and D.3. Furthermore, we also provide the detailed derivations of the theoretically recommended range of synchronization period $k \in \mathbb{N}$.

D.1 DERIVATION OF THEORETICALLY RECOMMENDED RANGE OF k IN EQUATION 12

We plug in $\sigma(\mathbf{A}) = \{1.195, 1.163, 1.094, 1.083, 1.018, 0.999, 0.969, 0.888, 0.879, 0.852\}$ with $\sigma_{max} = 1.195$ and $\sigma_{min} = 0.852$ to Theorem 5-8. Then we have

- LA-GD$_{\text{Alt}}$: $\{k \in \mathbb{N} : k \arccos(1 - \frac{0.1^2 \sigma_i^2}{2}) \bmod \pi \neq 0, \forall \sigma_i\}$,
- LA-GD$_{\text{Sim}}$: $\{k \in \mathbb{N} : k \arctan \eta\sigma_i \bmod \pi \neq 0, \forall \sigma_i\} \cap \left(\frac{\pi}{2 \arctan 0.08}, \frac{3\pi}{2 \arctan 0.12}\right)$,
- LA-EG$_{\text{Sim}}$: $\{k \in \mathbb{N} : k \arctan \frac{\eta\sigma_i}{1-\eta\sigma_i} \bmod \pi \neq 0, \forall \sigma_i\} \cap (\frac{\pi}{2 \arctan 0.09}, \frac{3\pi}{2 \arctan 0.13})$,

which give ranges for k as in TableD.2.

D.2 DERIVATION OF THEORETICALLY RECOMMENDED RANGE OF k IN EQUATION 13

LA-GD$_{\text{Alt}}$ From Equation 2, the Jacobian of dynamics $F_{\text{LA-GD}_{\text{Alt}}}$ of Equation 13 can be derived as

$$\nabla_{\mathbf{x}} F_{\text{GD}_{\text{Alt}}}(x_1, x_2) = \begin{bmatrix} 1 & -\eta \\ \eta & 1 - \eta^2 + \eta\epsilon(1 - 3x_2^2) \end{bmatrix} \begin{bmatrix} x_1 \\ x_2 \end{bmatrix}, \tag{21}$$

and it is trivial to see that it has an equilibrium at $(0, 0)$. By plugging in $\epsilon = 0.01$ and $\eta = 0.05$, we obtain

$$\nabla_{\mathbf{x}} F_{\text{GD}_{\text{Alt}}}(0, 0) = \begin{bmatrix} 1 & -0.05 \\ 0.05 & 0.998 \end{bmatrix} \tag{22}$$

with eigenvalues $\lambda_{\pm} \overset{\text{def}}{=} 0.99 \pm 0.05i$. Note that $|\lambda_{\pm}| = 1.0003 > 1$ and $\nabla_{\mathbf{x}} F_{\text{GD}_{\text{Alt}}}(0, 0)$ has the imaginary conditioning of 1, which implies that the origin is an unstable equilibrium of GD$_{\text{Alt}}$ that can be locally stabilized by a Lookahead dynamics. By plugging in the eigenvalues and $\theta_{min}(\nabla_{\mathbf{x}} F_{\text{GD}_{\text{Alt}}}(0, 0)) = \theta_{max}(\nabla_{\mathbf{x}} F_{\text{GD}_{\text{Alt}}}(0, 0)) = \arctan \frac{0.05}{0.99} = 0.0504$ to Theorem 10, we obtain the theoretically recommended range of k as $(31.16, 93.49)$.

LA-GD$_{\text{Sim}}$ From Equation 1, the Jacobian of dynamics $F_{\text{LA-GD}_{\text{Sim}}}$ of Equation 13 can be derived as

$$\nabla_{\mathbf{x}} F_{\text{GD}_{\text{Sim}}}(x_1, x_2) = \begin{bmatrix} 1 & -\eta \\ \eta & 1 + \eta\epsilon(1 - 3x_2^2) \end{bmatrix} \begin{bmatrix} x_1 \\ x_2 \end{bmatrix}, \tag{23}$$

and it is trivial to see that it has an equilibrium at $(0, 0)$. By plugging in $\epsilon = 0.01$ and $\eta = 0.05$, we obtain

$$\nabla_{\mathbf{x}} F_{\text{GD}_{\text{Sim}}}(0, 0) = \begin{bmatrix} 1 & -0.05 \\ 0.05 & 1.005 \end{bmatrix} \tag{24}$$

with eigenvalues $\lambda_{\pm} \overset{\text{def}}{=} 1.0025 \pm 0.0499i$. Note that $|\lambda_{\pm}| = 1.0037 > 1$ and $\nabla_{\mathbf{x}} F_{\text{GD}_{\text{Sim}}}(0, 0)$ has the imaginary conditioning of 1, which implies that the origin is an unstable equilibrium of GD$_{\text{Alt}}$ that can be locally stabilized by a Lookahead dynamics. By plugging in the eigenvalues and $\theta_{min}(\nabla_{\mathbf{x}} F_{\text{GD}_{\text{Sim}}}(0, 0)) = \theta_{max}(\nabla_{\mathbf{x}} F_{\text{GD}_{\text{Sim}}}(0, 0)) = \arctan \frac{0.0499}{1.0025} = 0.0497$ to Theorem 10, we obtain the theoretically recommended range of k as $(31.6, 94.81)$.

LA-EG$_{\text{Sim}}$ From Equation 5, the dynamics $F_{\text{LA-EG}_{\text{Sim}}}$ of Equation 13 can be derived as

$$\begin{bmatrix} x_1' \\ x_2' \end{bmatrix} = F_{\text{EG}_{\text{Sim}}}(x_1, x_2) = \begin{bmatrix} x_1 - \eta x_2' \\ x_2 + \eta(x_1' + \epsilon(x_2' - x_2'^3)) \end{bmatrix}. \tag{25}$$

We first show that $(0,0)$ is an equilibrium of $F_{\text{LA-EG}_{\text{Sim}}}$ for a small $\epsilon > 0$ and $\eta > 0$. By plugging in $x_1 = 0$ and $x_2 = 0$ to Equation 25 with some algebra, we get

$$(1 - \eta\epsilon + \eta^2)x_2' = -\eta\epsilon x_2'^3. \tag{26}$$

Suppose $x_2' \neq 0$. Then we have $x_2'^2 = \frac{1-\eta\epsilon+\eta^2}{-\eta\epsilon}$, which is impossible fo a small η and ϵ (*e.g.*, $\eta = 0.05$ and $\epsilon = 0.01$). Therefore we conclude $x_2' = 0$, from which follows that $x_1' = 0$, implying $(0,0)$ is an equilibrium of $F_{\text{EG}_{\text{Sim}}}$.

Now observe that Equation 25 can be rewritten as

$$x_1 = x_1' + \eta x_2', \tag{27}$$

$$x_2 = (1 - \eta\epsilon)x_2' + \eta\epsilon x_2'^3 - \eta x_1', \tag{28}$$

from which follows that

$$\nabla_{\mathbf{x}} F^{-1}{}_{\text{EG}_{\text{Sim}}}(0,0) = \begin{bmatrix} 1 & \eta \\ -\eta & 1 - \eta\epsilon \end{bmatrix}. \tag{29}$$

Then we can compute $\nabla_{\mathbf{x}} F_{\text{EG}_{\text{Sim}}}(0,0)$ using the inverse function theorem:

$$\nabla_{\mathbf{x}} F_{\text{EG}_{\text{Sim}}}(0,0) = (\nabla_{\mathbf{x}} F^{-1}{}_{\text{EG}_{\text{Sim}}}(0,0))^{-1} = \begin{bmatrix} 1 & \eta \\ -\eta & 1 - \eta\epsilon \end{bmatrix}^{-1}. \tag{30}$$

By plugging in $\epsilon = 0.01$ and $\eta = 0.05$, we obtain

$$\nabla_{\mathbf{x}} F_{\text{EG}_{\text{Sim}}}(0,0) = \begin{bmatrix} 0.9975 & -0.0499 \\ 0.0499 & 0.998 \end{bmatrix} \tag{31}$$

with eigenvalues $\lambda_{\pm} = 0.9978 \pm 0.0499i$. Note that $|\lambda_{\pm}| = 0.999 < 1$ and $\nabla_{\mathbf{x}} F_{\text{EG}_{\text{Sim}}}(0,0)$ has the imaginary conditioning of 1, which implies that the origin is an stable equilibrium of EG_{Sim} whose local convergence can be accelerated by a Lookahead dynamics. By plugging in the eigenvalues and $\theta_{min}(\nabla_{\mathbf{x}} F_{\text{EG}_{\text{Sim}}}(0,0)) = \theta_{max}(\nabla_{\mathbf{x}} F_{\text{EG}_{\text{Sim}}}(0,0)) = \arctan \frac{0.0499}{0.9978} = 0.0499$ to Theorem 11, we obtain the theoretically recommended range of k as $(31.47, 94.43)$.

Table D.2: Hyperparameters used for the experiment on the bilinear game

Configuration	**k (Theorem 5-8)**	**k**	**α (Theorem 5-8)**	**α**
LA-GD$_{\text{Alt}}{}^{+}$	$\mathbb{N}$	25	$(0,1)$	0.1
LA-GD$_{\text{Alt}}{}^{-}$	$\mathbb{N}$	5	$(0,1)$	0.9
LA-GD$_{\text{Sim}}{}^{+}$	$(18.47, 39.62)$	25	small enough	0.1
LA-GD$_{\text{Sim}}{}^{-}$	$(18.47, 39.62)$	5	small enough	0.9
LA-EG$_{\text{Sim}}{}^{+}$	$(16.9, 34.93)$	25	large enough	0.9
LA-EG$_{\text{Sim}}{}^{-}$	$(16.9, 34.93)$	5	large enough	0.1

Table D.3: Hyperparameters used for the experiment on the nonlinear game

Configuration	**k (Theorem 10, 11)**	**k**	**α (Theorem 10,11)**	**α**
LA-GD$_{\text{Alt}}{}^{+}$	$(31.16, 93.49)$	35	small enough	0.1
LA-GD$_{\text{Alt}}{}^{-}$	$(31.16, 93.49)$	5	small enough	0.9
LA-GD$_{\text{Sim}}{}^{+}$	$(31.6, 94.81)$	35	small enough	0.1
LA-GD$_{\text{Sim}}{}^{-}$	$(31.6, 94.81)$	5	small enough	0.9
LA-EG$_{\text{Sim}}{}^{+}$	$(31.47, 94.43)$	35	large enough	0.9
LA-EG$_{\text{Sim}}{}^{-}$	$(31.47, 94.43)$	5	large enough	0.1

E PROOFS

E.1 PROOF OF PROPOSITION 1

Proof. One can easily check from Equation 1 that the dynamics $F_{\text{GD}_{\text{Sim}}}$ can be written as

$$F_{\text{GD}_{\text{Sim}}}(x_1^{(t)}, x_2^{(t)}) = \begin{bmatrix} 1 & -\eta \\ \eta & 1 \end{bmatrix} \begin{bmatrix} x_1^{(t)} \\ x_2^{(t)} \end{bmatrix}. \tag{32}$$

Defining $\mathbf{M} \stackrel{\text{def}}{=} \begin{bmatrix} 1 & -\eta \\ \eta & 1 \end{bmatrix}$, its Lookahead dynamics $G_{\text{LA-GD}_{\text{Sim}}}$ can be written as

$$G_{\text{LA-GD}_{\text{Sim}}}(x_1^{(t)}, x_2^{(t)}) = ((1-\alpha)\mathbf{I} + \alpha\mathbf{M}^k) \begin{bmatrix} x_1^{(t)} \\ x_2^{(t)} \end{bmatrix}. \tag{33}$$

It follows that the eigenvalues of $\nabla_{\mathbf{x}} G_{\text{LA-GD}_{\text{Sim}}}$ can be written as $1 - \alpha + \alpha\lambda_\pm^k$ with $\lambda_\pm \stackrel{\text{def}}{=} 1 \pm i\eta \in \text{eig}(\mathbf{M})$. Now let us choose k such that $\lambda_\pm^k \notin \mathbb{R}$. Then, $(1-\alpha)\mathbf{I} + \alpha\mathbf{M}^k$ is diagonalizable as it admits complex conjugate eigenvalues $1 - \alpha + \alpha\lambda_\pm^k$. Furthermore, if we choose k such that satisfies $\Re(\lambda_\pm^k) < 1$, the line segment between $(1, 0)$ and $\lambda_\pm^k$ contains a line segment inside S_1 as in figure 1(b). Therefore, we can interpolate $1 - \alpha + \alpha\lambda_\pm^k$ inside S_1 by choosing small enough α for such k, implying $|1 - \alpha + \alpha\lambda_\pm^k| < 1$. We thus conclude from Lemma 14 that the iterates of $G_{\text{LA-GD}_{\text{Sim}}}$ converge to the Nash equilibrium $(0, 0)$ of the game. The proof for divergence of $F_{\text{GD}_{\text{Sim}}}$ follows from Lemma 14 and can be found in Gidel et al. (2019a). □

E.2 PROOF OF PROPOSITION 2 ON PP_{SIM}

Proof. Using simple algebra on Equation 4, the dynamics $F_{\text{PP}_{\text{Sim}}}$ can be written as

$$F_{\text{PP}_{\text{Sim}}}(x_1^{(t)}, x_2^{(t)}) = \frac{1}{1+\eta} \begin{bmatrix} 1 & -\eta \\ \eta & 1 \end{bmatrix} \begin{bmatrix} x_1^{(t)} \\ x_2^{(t)} \end{bmatrix}. \tag{34}$$

Defining $\mathbf{M} \stackrel{\text{def}}{=} \frac{1}{1+\eta} \begin{bmatrix} 1 & -\eta \\ \eta & 1 \end{bmatrix}$, its Lookahead dynamics $G_{\text{LA-PP}_{\text{Sim}}}$ with a synchronization period $k \in \mathbb{N}$ and a rate $\alpha \in (0, 1)$ can be written as

$$G_{\text{LA-PP}_{\text{Sim}}}(x_1^{(t)}, x_2^{(t)}) = ((1-\alpha)\mathbf{I} + \alpha\mathbf{M}^k) \begin{bmatrix} x_1^{(t)} \\ x_2^{(t)} \end{bmatrix}. \tag{35}$$

It follows that the eigenvalues of $\nabla_{\mathbf{x}} G_{\text{LA-PP}_{\text{Sim}}}$ are $1 - \alpha + \alpha\lambda_\pm^k$ with $\lambda_\pm \stackrel{\text{def}}{=} \frac{1 \pm i\eta}{1+\eta^2} \in \text{eig}(\mathbf{M})$. Now, let us choose k such that $\lambda_\pm^k \notin \mathbb{R}$. Then, $(1-\alpha)\mathbf{I} + \alpha\mathbf{M}^k$ is diagonalizable as it admits complex conjugate eigenvalues $1 - \alpha + \alpha\lambda_\pm^k$. Furthermore, we know that $1 - \alpha + \alpha\lambda_\pm^k$ is an interpolation between two distinct points on/inside S_1 since $|\lambda_\pm|^k < 1$ for any $\eta \in (0, 1)$. It follows that $|1 - \alpha + \alpha\lambda_\pm^k| < 1$, from which we conclude from Lemma 14 that the iterates of $G_{\text{LA-PP}_{\text{Sim}}}$ converge to the Nash equilibrium $(0, 0)$ of the game with convergence rate $\mathcal{O}(|1 - \alpha + \alpha\lambda_\pm^k|^{t/k})$, assuming the amortization of its computation over k forward steps.

Now we show that the convergence can be accelerated upon the base dynamics $F_{\text{PP}_{\text{Sim}}}$ if we carefully choose k and set α large enough. Figure 1(c) intuitively shows that the line segment between $(1, 0)$ and $\lambda_\pm^k$ contains a line segment inside $S_{|\lambda_\pm|^k}$ when k is such that $\Re(\lambda_\pm^k) < |\lambda_\pm^{2k}|$. Therefore, we can place the interpolation $1 - \alpha + \alpha\lambda_\pm^k$ inside $S_{|\lambda_\pm|^k}$ by choosing large enough α for such k. This shows that the convergence rate $\mathcal{O}(|1 - \alpha + \alpha\lambda_\pm^k|^{t/k})$ of $G_{\text{LA-PP}_{\text{Sim}}}$ can be accelerated upon the rate $\mathcal{O}(|\lambda_\pm|^t)$ of its base dynamics with a proper k and a large enough α, concluding the proof. □

E.3 PROOF OF PROPOSITION 2 ON EG_{SIM}

Proof. Using simple algebra on Equation 5, the dynamics $F_{\text{EG}_{\text{Sim}}}$ can be written as

$$F_{\text{EG}_{\text{Sim}}}(x_1^{(t)}, x_2^{(t)}) = \begin{bmatrix} 1-\eta^2 & -\eta \\ \eta & 1-\eta^2 \end{bmatrix} \begin{bmatrix} x_1^{(t)} \\ x_2^{(t)} \end{bmatrix}. \tag{36}$$

Defining $\mathbf{M} \stackrel{\text{def}}{=} \frac{1}{1+\eta}\begin{bmatrix} 1-\eta^2 & -\eta \\ \eta & 1-\eta^2 \end{bmatrix}$, its Lookahead dynamics $G_{\text{LA-EG}_{\text{Sim}}}$ with a synchronization period $k \in \mathbb{N}$ and a rate $\alpha \in (0,1)$ can be written as

$$G_{\text{LA-EG}_{\text{Sim}}}(x_1^{(t)}, x_2^{(t)}) = ((1-\alpha)\mathbf{I} + \alpha\mathbf{M}^k)\begin{bmatrix} x_1^{(t)} \\ x_2^{(t)} \end{bmatrix}. \tag{37}$$

It follows that the eigenvalues of $\nabla_{\mathbf{x}} G_{\text{LA-EG}_{\text{Sim}}}$ are $1-\alpha+\alpha\lambda_\pm^k$ with $\lambda_\pm \stackrel{\text{def}}{=} 1-\eta^2 \pm i\eta \in \text{eig}(\mathbf{M})$. Now, let us choose k such that $\lambda_\pm^k \notin \mathbb{R}$. Then, $(1-\alpha)\mathbf{I} + \alpha\mathbf{M}^k$ is diagonalizable as it admits complex conjugate eigenvalues $1-\alpha+\alpha\lambda_\pm^k$. Furthermore, we know that $1-\alpha+\alpha\lambda_\pm^k$ is an interpolation between two distinct points on/inside S_1 since $|\lambda_\pm|^k < 1$ for any $\eta \in (0,1)$. It follows that $|1-\alpha+\alpha\lambda_\pm^k| < 1$, from which we conclude from Lemma 14 that the iterates of $G_{\text{LA-EG}_{\text{Sim}}}$ converge to the Nash equilibrium $(0,0)$ of the game with convergence rate $\mathcal{O}(|1-\alpha+\alpha\lambda_\pm^k|^{t/k})$, assuming the amortization of its computation over k forward steps.

Now we show that the convergence can be accelerated upon the base dynamics $F_{\text{EG}_{\text{Sim}}}$ if we carefully choose k and set α large enough. Figure 1(c) intuitively shows that the line segment between $(1,0)$ and $\lambda_\pm^k$ contains a line segment inside $S_{|\lambda_\pm|^k}$ when k is such that $\Re(\lambda_\pm^k) < |\lambda_\pm^{2k}|$. Therefore, we can place the interpolation $1-\alpha+\alpha\lambda_\pm^k$ inside $C_{|\lambda_\pm|^k}$ by choosing large enough α for such k. This shows that convergence rate $\mathcal{O}(|1-\alpha+\alpha\lambda_\pm^k|^{t/k})$ of $G_{\text{LA-EG}_{\text{Sim}}}$ can be accelerated upon the rate $\mathcal{O}(|\lambda_\pm|^t)$ of its base dynamics with a proper k and a large enough α, concluding the proof for $G_{\text{LA-EG}_{\text{Sim}}}$. □

E.4 Proof of Theorem 3

Proof. We prove each of the cases in their order.

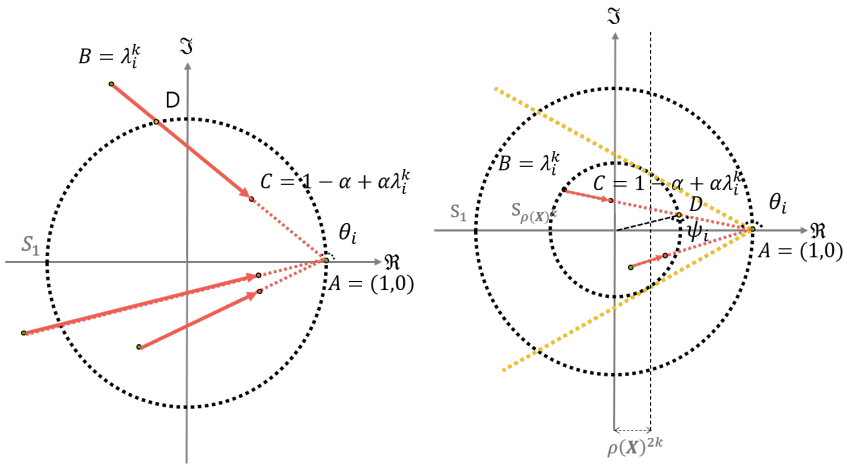

(a) $\rho(\mathbf{X}) > 1$ (b) $\rho(\mathbf{X}) < 1$

Figure 4: Visualized eigenvalues of $(1-\alpha)\mathbf{I} + \alpha\mathbf{X}^k$.

Case $\rho(\mathbf{X}) = 1$. Assume that ${\lambda_{\text{max}}}^k \neq 1$ for any $\lambda_{\text{max}} \in \text{eig}_{\text{max}}(\mathbf{X})$. Then we can immediately conclude $\rho(f(\mathbf{X})) < 1$ since $1-\alpha+\alpha\lambda_i^k \in \text{eig}(f(\mathbf{X}))$ is an interpolation between two distinct points $(1,0)$ and λ_i^k on/inside S_1 for any $\lambda_i \in \text{eig}(\mathbf{X})$.

Case $\rho(\mathbf{X}) > 1$. Assume that $\Re(\lambda_i^k) < 1$ for any $\lambda_i \in \text{eig}(\mathbf{X})$ and let $\lambda_i \in \text{eig}(\mathbf{X})$ be such that $|\lambda_i| > 1$. Then λ_i^k can be visualized as in Figure 4 (a), where the existence of D is guaranteed by $\Re(\lambda_i^k) < 1$. It is easy to see from the figure that

$$\left\|\overline{AC}\right\| = \alpha|\lambda_i^k - 1| < 2\cos(\pi - \theta_i) = \left\|\overline{AD}\right\| \tag{38}$$

is sufficient to place $1-\alpha+\alpha\lambda_i^k$ inside S_1. Furthermore, $1-\alpha+\alpha\lambda_i^k$ lies inside S_1 for any $\lambda_i \in \text{eig}(\mathbf{X})$ such that $|\lambda_i| \leq 1$ since $1-\alpha+\alpha\lambda_i^k$ is an interpolation between two distinct points on/inside S_1. Therefore we conclude $\rho(f(\mathbf{X})) < 1$.

Case $\rho(\mathbf{X}) < 1$. Assume that $\Re(\lambda_i^k) < \rho(\mathbf{X})^{2k}$ for any $\lambda_i \in \text{eig}(\mathbf{X})$. Then λ_i^k can be visualized as in Figure 4 since the existence of D is guaranteed by $\Re(\lambda_i^k) < \rho(\mathbf{X})^{2k}$ and $\sin(\phi_i) = \sin(\theta_i)/\rho(\mathbf{X})^k$ follows from the law of sines. Therefore we can intuitively see from the figure that

$$\left\|\overline{BC}\right\| = (1-\alpha)|\lambda_i^k - 1| < 2\rho(\mathbf{X})^k \cos(\pi - \phi_i) = \left\|\overline{BD}\right\| \tag{39}$$

is sufficient to place $1 - \alpha + \alpha\lambda_i^k$ inside $S_{\rho(X)^k}$, hence concluding the proof. □

E.5 Proof of Theorem 4

Proof. Let us denote $\theta_{min} \stackrel{\text{def}}{=} \theta_{min}(\mathbf{X})$, $\theta_{max} \stackrel{\text{def}}{=} \theta_{max}(\mathbf{X})$ for brevity and let $k \in \mathbb{N}$ be such that $k \in (\frac{\pi}{2\theta_{min}}, \frac{3\pi}{2\theta_{max}})$. Then we have $k\theta_{min} \in (\frac{\pi}{2}, \frac{3\pi\theta_{min}}{2\theta_{max}}) \subseteq (\frac{\pi}{2}, \frac{3\pi}{2})$ and $k\theta_{max} \in (\frac{\pi\theta_{max}}{2\theta_{min}}, \frac{3\pi}{2}) \subseteq (\frac{\pi}{2}, \frac{3\pi}{2})$, which implies $\Re(\lambda_i^k) < 0$ for any $\lambda_i \in \text{eig}(\mathbf{X})$ such that $\Im(\lambda_i) > 0$. Since any eigenvalues of $\mathbf{X}$ exist as complex conjugate pairs by the assumption on non-zero imaginary parts of $\text{eig}(\mathbf{J})$, we conclude $\Re(\lambda_i^k) < 0$ for any $\lambda_i \in \text{eig}(\mathbf{X})$.

Now we show that the existence of $k \in \mathbb{N}$ such that $k \in (\frac{\pi}{2\theta_{min}}, \frac{3\pi}{2\theta_{max}})$ is guaranteed for a small enough $\eta > 0$ when $\frac{\Im_{max}(\mathbf{J})}{\Im_{min}(\mathbf{J})} < 3$. Using simple algebra, we can see that $\theta_{max} < f(\theta_{min})$ for $f : \mathbb{R} \to \mathbb{R}$ defined by $f(x) = \frac{3\pi x}{\pi + 2x}$ is equivalent to $\frac{\pi}{2\theta_{min}} - \frac{3\pi}{2\theta_{max}} > 1$, implying nonempty $\mathbb{N} \cap (\frac{\pi}{2\theta_{min}}, \frac{3\pi}{2\theta_{max}})$. Therefore it suffices to show that $\theta_{max} < f(\theta_{min})$ holds for a small enough $\eta > 0$ when $\frac{\Im_{max}(\mathbf{J})}{\Im_{min}(\mathbf{J})} < 3$.

Let us define a function $H : \mathbb{R} \times \mathbb{M}_{m\times m} \to \mathbb{R}$ given by

$$H(\eta, \mathbf{J}) \stackrel{\text{def}}{=} \left(1 + \frac{2\theta_{max}^+}{\pi}\right)\left(\frac{1 + \eta\Re_{max}(\mathbf{J})}{1 + \eta\Re_{min}(\mathbf{J})}\right)\left(\frac{1 + 2\sec\theta_{min}^-}{1 + 2\sec\theta_{max}^+} + b\right), \tag{40}$$

where $\theta_{min}^- \stackrel{\text{def}}{=} \arctan\frac{\eta\Im_{min}(\mathbf{J})}{1+\eta\Re_{max}(\mathbf{J})}$, $\theta_{max}^+ \stackrel{\text{def}}{=} \arctan\frac{\eta\Im_{max}(\mathbf{J})}{1+\eta\Re_{min}(\mathbf{J})}$ and $b \stackrel{\text{def}}{=} \frac{(1+2\sec\theta_{min}^-)\tan^4\theta_{max}^+}{540}$.

We show that the inequality

$$\frac{\Im_{max}(\mathbf{J})}{\Im_{min}(\mathbf{J})} < \frac{3}{H(\eta, \mathbf{J})} \tag{41}$$

implies $\theta_{max} < f(\theta_{min})$ and conclude the proof by showing that there exists a small enough $\eta > 0$ such that satisfies Equation 41 when $\frac{\Im_{max}(\mathbf{J})}{\Im_{min}(\mathbf{J})} < 3$.

Note that the inequalities $\theta_{min}^- \leq \theta_{min}$ and $\theta_{max} \leq \theta_{max}^+$ directly follow from the definitions of θ_{min}^- and θ_{max}^+. Furthermore, using the Shafer-type double inequalities (Mortici & Srivastava, 2014) for $\arctan(\cdot)$, we obtain

$$\theta_{min}^- \geq \frac{3\tan\theta_{min}^-}{1 + 2\sqrt{1 + \tan^2\theta_{min}^-}} = \frac{3\eta\Im_{min}}{(1 + \eta\Re_{max})(1 + 2\sec\theta_{min}^-)}, \tag{42}$$

$$\theta_{max}^+ \leq \frac{3\tan\theta_{max}^+}{1 + 2\sqrt{1 + \tan^2\theta_{max}^+}} + \frac{1}{180}\tan^5\theta_{max}^+ \tag{43}$$

$$= \frac{3\eta\Im_{max}}{(1 + \eta\Re_{min})(1 + 2\sec\theta_{max}^+)} + \frac{\eta\Im_{max} tan^4\theta_{max}^+}{180(1 + \eta\Re_{min})}, \tag{44}$$

from which follows that

$$\frac{\theta_{max}}{\theta_{min}} \leq \frac{\theta_{max}^+}{\theta_{min}^-} = \frac{\Im_{max}(\mathbf{J})}{\Im_{min}(\mathbf{J})}\left(\frac{1 + \eta\Re_{max}(\mathbf{J})}{1 + \eta\Re_{min}(\mathbf{J})}\right)\left(\frac{1 + 2\sec\theta_{min}^-}{1 + 2\sec\theta_{max}^+} + b\right). \tag{45}$$

However, assuming inequality 41, we can derive

$$\frac{\Im_{max}(\mathbf{J})}{\Im_{min}(\mathbf{J})}\left(\frac{1 + \eta\Re_{max}(\mathbf{J})}{1 + \eta\Re_{min}(\mathbf{J})}\right)\left(\frac{1 + 2\sec\theta_{min}^-}{1 + 2\sec\theta_{max}^+} + b\right) < \frac{3\pi}{\pi + 2\theta_{max}^+} = \frac{f(\theta_{max}^+)}{\theta_{max}^+}. \tag{46}$$

Furthermore, since $f'(x) = \frac{3\pi^2}{(\pi+2x)^2}$, we have concavity of f. Hence it follows that

$$\frac{f(\theta_{max}^+)}{\theta_{max}^+} < \frac{f(\theta_{min})}{\theta_{min}}, \tag{47}$$

from which we obtain $\theta_{max} < f(\theta_{min})$ by combining Equation 45-47.

Finally, we prove that Equation 41 holds for a small enough $\eta > 0$ when $\frac{\Im_{max}(\mathbf{J})}{\Im_{min}(\mathbf{J})} < 3$. Assume $\frac{\Im_{max}(\mathbf{J})}{\Im_{min}(\mathbf{J})} < 3$ and let $\epsilon \overset{\text{def}}{=} 3 - \frac{\Im_{max}(\mathbf{J})}{\Im_{min}(\mathbf{J})} > 0$. By the continuity of $\frac{3}{H(\cdot,\mathbf{J})}$ at $\eta = 0$ and the fact that $H(0,\mathbf{J}) = 1$, there exists $\delta > 0$ such that $|3 - \frac{3}{H(\eta,\mathbf{J})}| < \epsilon$ holds for any $\eta \in (0,\delta)$. Therefore we have $\frac{\Im_{max}(\mathbf{J})}{\Im_{min}(\mathbf{J})} = 3 - \epsilon < \frac{3}{H(\eta,\mathbf{J})}$ for any $\eta \in (0,\delta)$, concluding the proof. □

E.6 Proof of Theorem 5

Proof. From Equation 2, the dynamics $F_{\text{GD}_{\text{Alt}}}$ of Equation 11 can be derived as

$$F_{\text{GD}_{\text{Alt}}}(\mathbf{x}_1^{(t)}, \mathbf{x}_2^{(t)}) = \begin{bmatrix} \mathbf{I}_r & -\eta\Sigma_r \\ \eta\Sigma_r & \mathbf{I}_r - \eta^2\Sigma_r^2 \end{bmatrix} \begin{bmatrix} \mathbf{x}_1^{(t)} \\ \mathbf{x}_2^{(t)} \end{bmatrix}. \tag{48}$$

Defining $\mathbf{M} \overset{\text{def}}{=} \begin{bmatrix} \mathbf{I}_r & -\eta\Sigma_r \\ \eta\Sigma_r & \mathbf{I}_r - \eta^2\Sigma_r^2 \end{bmatrix}$, its Lookahead dynamics $G_{\text{LA-GD}_{\text{Alt}}}$ with a synchronization period $k \in \mathbb{N}$ and a rate $\alpha \in (0,1)$ can be written as

$$G_{\text{LA-GD}_{\text{Alt}}}(\mathbf{x}_1^{(t)}, \mathbf{x}_2^{(t)}) = ((1-\alpha)\mathbf{I} + \alpha\mathbf{M}^k) \begin{bmatrix} \mathbf{x}_1^{(t)} \\ \mathbf{x}_2^{(t)} \end{bmatrix}. \tag{49}$$

Together with Equation 14, we can see that eigenvalues of $\nabla_{\mathbf{x}} G_{\text{LA-GD}_{\text{Alt}}}$ can be written as $1-\alpha+\alpha\lambda_{\pm i}^k$ with $\lambda_{\pm i} \overset{\text{def}}{=} 1 - \frac{\eta^2\sigma_i^2}{2} \pm i\eta\sigma_i\sqrt{1 - \frac{\eta^2\sigma_i^2}{4}} \in \text{eig}(\mathbf{M})$ for any $\eta \in \left(0, \frac{2}{\sigma_{max}}\right)$. In the meanwhile, simple calculation gives us $|\lambda_{\pm i}| = 1$, which implies $\rho(\mathbf{M}) = 1$. Now assume $k \in \mathbb{N}$ is such that $k \arccos(1 - \frac{\eta^2\sigma_i^2}{2}) \bmod \pi \neq 0$ for any σ_i. Then it follows that $\lambda_{\pm i}^k \neq 1$ for any $\lambda_{\pm i} \in \text{eig}(\mathbf{M})$. Therefore we have $\rho(\nabla_{\mathbf{x}} G_{\text{LA-GD}_{\text{Alt}}}) < 1$ by Theorem 3. Furthermore, $\nabla_{\mathbf{x}} G_{\text{LA-GD}_{\text{Alt}}}$ is diagonalizable as it admits complex conjugate eigenvalues $1 - \alpha + \alpha\lambda_{\pm i}^k$. It follows from Lemma 14 that the iterates converges to the origin. We conclude the proof by observing that the transformations $\mathbf{x}_1 \mapsto \mathbf{U}[\mathbf{x}_1; \mathbf{0}_{m-r}] + \mathbf{x}_1^*$ and $\mathbf{x}_2 \mapsto \mathbf{V}[\mathbf{x}_2; \mathbf{0}_{n-r}] + \mathbf{x}_2^*$ of $(\mathbf{0}, \mathbf{0}) \in \mathbb{R}^r \times \mathbb{R}^r$ gives $(\mathbf{x}_1^*, \mathbf{x}_2^*) \in \mathbb{R}^m \times \mathbb{R}^n$, which is a Nash equilibrium of Equation 9. □

E.7 Proof of Theorem 6

Proof. From Equation 1, the dynamics $F_{\text{GD}_{\text{Sim}}}$ of Equation 11 can be derived as

$$F_{\text{GD}_{\text{Sim}}}(\mathbf{x}_1^{(t)}, \mathbf{x}_2^{(t)}) = \begin{bmatrix} \mathbf{I}_r & -\eta\Sigma_r \\ \eta\Sigma_r & \mathbf{I}_r \end{bmatrix} \begin{bmatrix} \mathbf{x}_1^{(t)} \\ \mathbf{x}_2^{(t)} \end{bmatrix}. \tag{50}$$

Let us define $\mathbf{J} \overset{\text{def}}{=} \begin{bmatrix} \mathbf{0}_r & \Sigma_r \\ -\Sigma_r & \mathbf{0}_r \end{bmatrix}$ and $\mathbf{M} \overset{\text{def}}{=} \mathbf{I} - \eta\mathbf{J}$. Then its Lookahead dynamics $G_{\text{LA-GD}_{\text{Sim}}}$ with a synchronization period $k \in \mathbb{N}$ and a rate $\alpha \in (0,1)$ can be written as

$$G_{\text{LA-GD}_{\text{Sim}}}(\mathbf{x}_1^{(t)}, \mathbf{x}_2^{(t)}) = ((1-\alpha)\mathbf{I} + \alpha\mathbf{M}^k) \begin{bmatrix} \mathbf{x}_1^{(t)} \\ \mathbf{x}_2^{(t)} \end{bmatrix}. \tag{51}$$

Together with Equation 15, we can see that the eigenvalues of $\nabla_{\mathbf{x}} G_{\text{LA-GD}_{\text{Sim}}}$ can be written as $1 - \alpha + \alpha\lambda_{\pm i}^k$ with $\lambda_{\pm i} \overset{\text{def}}{=} 1 \pm i\eta\sigma_i \in \text{eig}(\mathbf{M})$. In the meanwhile, one can easily see that $|\lambda_{\pm i}| > 1$, implying $\rho(\mathbf{M}) > 1$. Now assume that $k \arctan \eta\sigma_i \bmod \pi \neq 0$ for any σ_i, $k \in \left(\frac{\pi}{2\arctan\eta\sigma_{min}}, \frac{3\pi}{2\arctan\eta\sigma_{max}}\right)$ and $\frac{\sigma_{max}}{\sigma_{min}} < 3$. Then since $\tan\theta_{min}(\mathbf{M}) = \eta\sigma_{min}$ and $\tan\theta_{max}(\mathbf{M}) = \eta\sigma_{max}$, we have $k \in (\frac{\pi}{2\theta_{min}(\mathbf{M})}, \frac{3\pi}{2\theta_{max}(\mathbf{M})})$. It follows from Theorem 4 that

$\Re(\lambda_{\pm i}^k) < 0$ for any $\lambda_{\pm i} \in \text{eig}(\mathbf{M})$, where the existence of such k is guaranteed for a small enough η since $\frac{\Im_{max}(\mathbf{J})}{\Im_{min}(\mathbf{J})} = \frac{\sigma_{max}}{\sigma_{min}} < 3$. Then it follows from Theorem 3 that $\rho(\nabla_{\mathbf{x}} G_{\text{LA-GD}_{\text{Sim}}}) < 1$ holds for a small enough α. Furthermore, $k \arctan \eta\sigma_i \bmod \pi \neq 0$ implies $\lambda_{\pm i}^k \notin \mathbb{R}$ and thus $\nabla_{\mathbf{x}} G_{\text{LA-GD}_{\text{Sim}}}$ is diagonalizable. Therefore, by Lemma 14, the iterates converges to the origin. We conclude the proof by observing that the transformations $\mathbf{x}_1 \mapsto \mathbf{U}[\mathbf{x}_1; \mathbf{0}_{m-r}] + \mathbf{x}_1^*$ and $\mathbf{x}_2 \mapsto \mathbf{V}[\mathbf{x}_2; \mathbf{0}_{n-r}] + \mathbf{x}_2^*$ of $(\mathbf{0}, \mathbf{0}) \in \mathbb{R}^r \times \mathbb{R}^r$ gives $(\mathbf{x}_1^*, \mathbf{x}_2^*) \in \mathbb{R}^m \times \mathbb{R}^n$, which is a Nash equilibrium of Equation 9. □

E.8 Proof of Theorem 7

Proof. From Equation 4, the dynamics $F_{\text{PP}_{\text{Sim}}}$ of Equation 11 can be derived as

$$F_{\text{PP}_{\text{Sim}}}(\mathbf{x}_1^{(t)}, \mathbf{x}_2^{(t)}) = \begin{bmatrix} \mathbf{I}_r & \eta\Sigma_r \\ -\eta\Sigma_r & \mathbf{I}_r \end{bmatrix}^{-1} \begin{bmatrix} \mathbf{x}_1^{(t)} \\ \mathbf{x}_2^{(t)} \end{bmatrix}. \tag{52}$$

Let us define $\mathbf{J} \stackrel{\text{def}}{=} \begin{bmatrix} \mathbf{0}_r & \Sigma_r \\ -\Sigma_r & \mathbf{0}_r \end{bmatrix}$ and $\mathbf{M} \stackrel{\text{def}}{=} (\mathbf{I} + \eta\mathbf{J})^{-1}$. Then its Lookahead dynamics $G_{\text{LA-GD}_{\text{Sim}}}$ with a synchronization period $k \in \mathbb{N}$ and a rate $\alpha \in (0, 1)$ can be written as

$$G_{\text{LA-GD}_{\text{Sim}}}(\mathbf{x}_1^{(t)}, \mathbf{x}_2^{(t)}) = ((1-\alpha)\mathbf{I} + \alpha\mathbf{M}^k) \begin{bmatrix} \mathbf{x}_1^{(t)} \\ \mathbf{x}_2^{(t)} \end{bmatrix}. \tag{53}$$

Together with Equation 16, we can see that the eigenvalues of $\nabla_{\mathbf{x}} G_{\text{LA-EG}_{\text{Sim}}}$ can be written as $1-\alpha+\alpha\lambda_{\pm i}^k$ with $\lambda_{\pm i} \stackrel{\text{def}}{=} \frac{1+i\eta\sigma_i}{1+\eta^2\sigma_i^2} \in \text{eig}(\mathbf{M})$. In the meanwhile, we can easily see that $|\lambda_{\pm i}| < 1$ for any $\eta > 0$, implying $\rho(\mathbf{M}) < 1$. Therefore, $1-\alpha+\alpha\lambda_{\pm i}^k$ is an interpolation between two distinct points $(1, 0)$ and $\lambda_{\pm i}^k$ on/inside S_1, implying $\rho(\nabla_{\mathbf{x}} G_{\text{LA-EG}_{\text{Sim}}}) < 1$. Now assume that $k \arctan \eta\sigma_i \bmod \pi \neq 0$ for any σ_i. Then $\nabla_{\mathbf{x}} G_{\text{LA-EG}_{\text{Sim}}}$ is diagonalizable since $k \arctan \eta\sigma_i \bmod \pi \neq 0$ implies $\lambda_{\pm i}^k \notin \mathbb{R}$. It follows from Lemma 14 that the iterates converges to the origin. However, the transformations $\mathbf{x}_1 \mapsto \mathbf{U}[\mathbf{x}_1; \mathbf{0}_{m-r}] + \mathbf{x}_1^*$ and $\mathbf{x}_2 \mapsto \mathbf{V}[\mathbf{x}_2; \mathbf{0}_{n-r}] + \mathbf{x}_2^*$ of $(\mathbf{0}, \mathbf{0}) \in \mathbb{R}^r \times \mathbb{R}^r$ gives $(\mathbf{x}_1^*, \mathbf{x}_2^*) \in \mathbb{R}^m \times \mathbb{R}^n$, which is a Nash equilibrium of Equation 9.

Now we show that $G_{\text{LA-PP}_{\text{Sim}}}$ can accelerate the convergence upon its base dynamics $F_{\text{PP}_{\text{Sim}}}$. Assume that $k \in \left(\frac{\pi}{2\arctan \eta\sigma_{min}}, \frac{3\pi}{2\arctan \eta\sigma_{max}}\right)$ and $\frac{\sigma_{max}}{\sigma_{min}} < 3$. Note that $\mathbf{M}^{-1}$ shares the same eigenvalues with the Jacobian of $F_{\text{GD}_{\text{Sim}}}$. Therefore we have $\tan\theta_{min}(\mathbf{M}^{-1}) = \eta\sigma_{min}$ and $\tan\theta_{max}(\mathbf{M}^{-1}) = \eta\sigma_{max}$, which implies $k \in \left(\frac{\pi}{2\theta_{min}(\mathbf{M}^{-1})}, \frac{3\pi}{2\theta_{max}(\mathbf{M}^{-1})}\right)$. It follows from Theorem 4 that $\Re(\lambda_{\pm i}^{-k}) < 0$ for any $\lambda_{\pm i}^{-1} \in \text{eig}(\mathbf{M}^{-1})$, where the existence of such k is guaranteed for a small enough η since $\frac{\Im_{max}(\mathbf{J})}{\Im_{min}(\mathbf{J})} = \frac{\sigma_{max}}{\sigma_{min}} < 3$. Then we have $\Re(\lambda_{\pm i}^k) < 0$ for any $\lambda_{\pm i} \in \text{eig}(\mathbf{M})$ since the reciprocal of a complex number preserves sign of the real part. Then it follows from Theorem 3 that $\rho(\nabla_{\mathbf{x}} G_{\text{LA-EG}_{\text{Sim}}}) < \rho(\mathbf{M})^k$ holds for a large enough α. We conclude the proof by using Lemma 14 and noting that the convergence rate $\mathcal{O}(\rho(\nabla_{\mathbf{x}} G_{\text{LA-PP}_{\text{Sim}}})^{\frac{t}{k}})$ of $G_{\text{LA-PP}_{\text{Sim}}}$ is faster than the rate $\mathcal{O}(\rho(\mathbf{M})^t)$ of $F_{\text{PP}_{\text{Sim}}}$, assuming amortization of computations over k forward steps. □

E.9 Proof of Theorem 8

Proof. From Equation 5, the dynamics $F_{\text{EG}_{\text{Sim}}}$ of Equation 11 can be derived as

$$F_{\text{EG}_{\text{Sim}}}(\mathbf{x}_1^{(t)}, \mathbf{x}_2^{(t)}) = \begin{bmatrix} \mathbf{I}_r - \eta\Sigma_r^2 & -\eta\Sigma_r \\ \eta\Sigma_r & \mathbf{I}_r - \eta\Sigma_r^2 \end{bmatrix} \begin{bmatrix} \mathbf{x}_1^{(t)} \\ \mathbf{x}_2^{(t)} \end{bmatrix}. \tag{54}$$

Let us define $\mathbf{J} \stackrel{\text{def}}{=} \begin{bmatrix} \Sigma_r^2 & \Sigma_r \\ -\Sigma_r & \Sigma_r^2 \end{bmatrix}$ and $\mathbf{M} \stackrel{\text{def}}{=} \mathbf{I} - \eta\mathbf{J}$. Then its Lookahead dynamics $G_{\text{LA-GD}_{\text{Sim}}}$ with a synchronization period $k \in \mathbb{N}$ and a rate $\alpha \in (0, 1)$ can be written as

$$G_{\text{LA-GD}_{\text{Sim}}}(\mathbf{x}_1^{(t)}, \mathbf{x}_2^{(t)}) = ((1-\alpha)\mathbf{I} + \alpha\mathbf{M}^k) \begin{bmatrix} \mathbf{x}_1^{(t)} \\ \mathbf{x}_2^{(t)} \end{bmatrix}. \tag{55}$$

Together with Equation 18, we can see that the eigenvalues of $\nabla_{\mathbf{x}} G_{\text{LA-EG}_{\text{Sim}}}$ can be written as $1-\alpha+\alpha\lambda_{\pm i}^k$ with $\lambda_{\pm i} \stackrel{\text{def}}{=} 1-\eta\sigma_i \pm i\eta\sigma_i \in \text{eig}(\mathbf{M})$. In the meanwhile, we can easily see that $|\lambda_{\pm i}| < 1$ for any $\eta \in \left(0, \frac{1}{\sigma_{max}}\right)$, implying $\rho(\mathbf{M}) < 1$. Therefore, $1-\alpha+\alpha\lambda_{\pm i}^k$ is an interpolation between two distinct points $(1,0)$ and $\lambda_{\pm i}^k$ on/inside S_1, implying $\rho(\nabla_{\mathbf{x}} G_{\text{LA-EG}_{\text{Sim}}}) < 1$. Now assume that $k \arctan \frac{\eta\sigma_i}{1-\eta\sigma_i} \bmod \pi \neq 0$ for any σ_i. Then $\nabla_{\mathbf{x}} G_{\text{LA-EG}_{\text{Sim}}}$ is diagonalizable since $k \arctan \frac{\eta\sigma_i}{1-\eta\sigma_i} \bmod \pi \neq 0$ implies $\lambda_{\pm i}^k \notin \mathbb{R}$. It follows from Lemma 14 that the iterates converges to the origin. However, the transformations $\mathbf{x}_1 \mapsto \mathbf{U}\left[\mathbf{x}_1; \mathbf{0}_{m-r}\right] + \mathbf{x}_1^*$ and $\mathbf{x}_2 \mapsto \mathbf{V}\left[\mathbf{x}_2; \mathbf{0}_{n-r}\right] + \mathbf{x}_2^*$ on $(\mathbf{0}, \mathbf{0}) \in \mathbb{R}^r \times \mathbb{R}^r$ gives $(\mathbf{x}_1^*, \mathbf{x}_2^*) \in \mathbb{R}^m \times \mathbb{R}^n$, which is a Nash equilibrium of Equation 9.

Now we show that $G_{\text{LA-EG}_{\text{Sim}}}$ can accelerate the convergence upon its base dynamics $F_{\text{EG}_{\text{Sim}}}$. Assume that $k \in \left(\frac{\pi}{2\arctan\frac{\eta\sigma_{min}}{1-\eta\sigma_{min}}}, \frac{3\pi}{2\arctan\frac{\eta\sigma_{max}}{1-\eta\sigma_{max}}}\right)$ and $\frac{\sigma_{max}}{\sigma_{min}} < 3$. Then we have $k \in \left(\frac{\pi}{2\theta_{min}(\mathbf{M})}, \frac{3\pi}{2\theta_{max}(\mathbf{M})}\right)$. It follows from Theorem 4 that $\Re(\lambda_{\pm i}^k) < 0$ for any $\lambda_{\pm i} \in \text{eig}(\mathbf{M})$, where the existence of such k is guaranteed for a small enough η since $\frac{\Im_{max}(\mathbf{J})}{\Im_{min}(\mathbf{J})} = \frac{\sigma_{max}}{\sigma_{min}} < 3$. Then it follows from Theorem 3 that $\rho(\nabla_{\mathbf{x}} G_{\text{LA-EG}_{\text{Sim}}}) < \rho(\mathbf{M})^k$ holds for a large enough α. We conclude the proof by using Lemma 14 and noting that the convergence rate $\mathcal{O}(\rho(\nabla_{\mathbf{x}} G_{\text{LA-EG}_{\text{Sim}}})^{\frac{t}{k}})$ of $G_{\text{LA-EG}_{\text{Sim}}}$ is faster than the rate $\mathcal{O}(\rho(\mathbf{M})^t)$ of $F_{\text{EG}_{\text{Sim}}}$, assuming amortization of computations over k forward steps. □

E.10 Proof of Theorem 9

Proof. From Equation 7, the Jacobian of G evaluated at $\mathbf{x}^*$ can written as

$$\nabla_{\mathbf{x}} G(\mathbf{x}^*) = \nabla_{\mathbf{x}}\left((1-\alpha)\text{id} + \alpha F^k\right)(\mathbf{x}^*) = (1-\alpha)\mathbf{I} + \alpha\nabla_{\mathbf{x}} F^k(\mathbf{x}^*) \tag{56}$$

$$= (1-\alpha)\mathbf{I} + \alpha\prod_{i=1}^{k}\nabla_{\mathbf{x}} F(F^{i-1}(\mathbf{x}^*)) = (1-\alpha)\mathbf{I} + \alpha(\nabla_{\mathbf{x}} F(\mathbf{x}^*))^k, \tag{57}$$

where the chain rule is used in third equality with a slight abuse of notation $F^0 \stackrel{\text{def}}{=} \text{id}$. We use the fact that $\mathbf{x}^*$ is an equilibrium of dynamics F for the last equality. It is easy to see from Equation 57 that eigenvalues of $\nabla_{\mathbf{x}} G(\mathbf{x}^*)$ can be written as $1-\alpha+\alpha\lambda_i^k$ for each $\lambda_i \in \text{eig}(\nabla_{\mathbf{x}} F(\mathbf{x}^*))$.

However, λ_i^k is either on/inside S_1 since $|\lambda_i| \leq 1$ for each i due to the asymptotic stability of $\mathbf{x}^*$ in F. Therefore, $1-\alpha+\alpha\lambda_i^k$ is an interpolation between two points $(1,0) \in S_1$ and λ_i^k either on/inside S_1; hence $|1-\alpha+\alpha\lambda_i^k| \leq 1$. By assumption that $\lambda_i^k \neq (1,0)$ for each $\lambda_i \in \text{eig}(\nabla_{\mathbf{x}} F(\mathbf{x}^*))$, the inequality is strict, *i.e.* $|1-\alpha+\alpha\lambda_i^k| < 1$, implying the local asymptotic stability of $\mathbf{x}^*$ in G by Proposition 13. □

E.11 Proof of Theorem 10

Proof. From Equation 7, the Jacobian of G evaluated at $\mathbf{x}^*$ can written as

$$\nabla_{\mathbf{x}} G(\mathbf{x}^*) = \nabla_{\mathbf{x}}\left((1-\alpha)\text{id} + \alpha F^k\right)(\mathbf{x}^*) = (1-\alpha)\mathbf{I} + \alpha\nabla_{\mathbf{x}} F^k(\mathbf{x}^*) \tag{58}$$

$$= (1-\alpha)\mathbf{I} + \alpha\prod_{i=1}^{k}\nabla_{\mathbf{x}} F(F^{i-1}(\mathbf{x}^*)) = (1-\alpha)\mathbf{I} + \alpha(\nabla_{\mathbf{x}} F(\mathbf{x}^*))^k, \tag{59}$$

where the chain rule is used in third equality with a slight abuse of notation $F^0 \stackrel{\text{def}}{=} \text{id}$. We use the fact that $\mathbf{x}^*$ is an equilibrium of dynamics F for the last equality.

Now assume that $\frac{\Im_{max}(\mathbf{J})}{\Im_{min}(\mathbf{J})} < 3$ and every eigenvalue of $\mathbf{J}$ has non-zero imaginary part. Then the existence of $k \in \mathbb{N}$ such that $k \in \left(\frac{\pi}{2\theta_{min}(\nabla_{\mathbf{x}} F(\mathbf{x}^*))}, \frac{3\pi}{2\theta_{max}(\nabla_{\mathbf{x}} F(\mathbf{x}^*))}\right)$ is guaranteed for a small enough η by Theorem 4. Furthermore, for such k, we have $\Re(\lambda_i^k) < 0$ for any $\lambda_i \in \text{eig}(\nabla_{\mathbf{x}} F(\mathbf{x}^*))$. Then it follows from the second case of Theorem 3 that $\rho(\nabla_{\mathbf{x}} G(\mathbf{x}^*)) < 1$ holds for a small enough α. By Proposition 13, this implies local asymptotic stability of $\mathbf{x}^*$ in G, concluding the proof. □

E.12 PROOF OF THEOREM 11

Proof. From Equation 7, the Jacobian of G evaluated at $\mathbf{x}^*$ can written as

$$\nabla_{\mathbf{x}} G(\mathbf{x}^*) = \nabla_{\mathbf{x}} \left((1-\alpha)\mathrm{id} + \alpha F^k\right)(\mathbf{x}^*) = (1-\alpha)\mathbf{I} + \alpha \nabla_{\mathbf{x}} F^k(\mathbf{x}^*) \tag{60}$$

$$= (1-\alpha)\mathbf{I} + \alpha \prod_{i=1}^{k} \nabla_{\mathbf{x}} F(F^{i-1}(\mathbf{x}^*)) = (1-\alpha)\mathbf{I} + \alpha(\nabla_{\mathbf{x}} F(\mathbf{x}^*))^k, \tag{61}$$

where the chain rule is used in third equality with a slight abuse of notation $F^0 \stackrel{\text{def}}{=} \mathrm{id}$. We use the fact that $\mathbf{x}^*$ is an equilibrium of dynamics F for the last equality.

Now assume that $\frac{\Im_{max}(\mathbf{J})}{\Im_{min}(\mathbf{J})} < 3$ and every eigenvalue of $\mathbf{J}$ has non-zero imaginary part. Then the existence of $k \in \mathbb{N}$ such that $k \in \left(\frac{\pi}{2\theta_{min}(\nabla_{\mathbf{x}} F(\mathbf{x}^*))}, \frac{3\pi}{2\theta_{max}(\nabla_{\mathbf{x}} F(\mathbf{x}^*))}\right)$ is guaranteed for a small enough η by Theorem 4. Furthermore, for such k, we have $\Re(\lambda_i^k) < 0$ for any $\lambda_i \in \mathrm{eig}(\nabla_{\mathbf{x}} F(\mathbf{x}^*))$. Then it follows from the third case of Theorem 3 that $\rho(\nabla_{\mathbf{x}} G(\mathbf{x}^*)) < \rho(\nabla_{\mathbf{x}} F(\mathbf{x}^*))^k$ holds for a small enough α. We conclude the proof by noting that this implies the upper bound $\mathcal{O}(\rho(\nabla_{\mathbf{x}} G(\mathbf{x}^*)^{\frac{t}{k}})$ on the rate of local convergence provided by Proposition 13 is faster than $\mathcal{O}(\nabla_{\mathbf{x}} F(\mathbf{x}^*)^t)$. □

E.13 PROOF OF THEOREM 12

Proof. We directly follow the proofs of Lemma 2.1 and Lemma 3.1 in Daskalakis & Panageas (2018) and show that $\alpha \in (0, \frac{1}{1+L^k})$ guarantees locally diffeomorphic Lookahead dynamics, *i.e.*, it is locally invertible at any given points.

Note from Equation 7 that the Jacobian of G evaluated at $\mathbf{x}$ can written as

$$\nabla_{\mathbf{x}} G(\mathbf{x}) = \nabla_{\mathbf{x}} \left((1-\alpha)\mathrm{id} + \alpha F^k\right)(\mathbf{x}) = (1-\alpha)\mathbf{I} + \alpha \nabla_{\mathbf{x}} F^k(\mathbf{x}) \tag{62}$$

$$= (1-\alpha)\mathbf{I} + \alpha \prod_{i=1}^{k} \nabla_{\mathbf{x}} F_{\mathcal{A}}(F^{i-1}(\mathbf{x})), \tag{63}$$

where we have used the chain rule in the last equality with a slight abuse of notation $F^0 \stackrel{\text{def}}{=} \mathrm{id}$.

Now assume that $\alpha \in \left(0, \frac{1}{1+L^k}\right)$ and consider the following inequalities

$$\rho(\prod_{i=1}^{k} \nabla_{\mathbf{x}} F_{\mathcal{A}}(F_{\mathcal{A}}^{i-1}(\mathbf{x}))) \leq \left\| \prod_{i=1}^{k} \nabla_{\mathbf{x}} F_{\mathcal{A}}(F_{\mathcal{A}}^{i-1}(\mathbf{x})) \right\| \leq \prod_{i=1}^{k} \left\| \nabla_{\mathbf{x}} F_{\mathcal{A}}(F_{\mathcal{A}}^{i-1}(\mathbf{x})) \right\| \leq L^k, \tag{64}$$

where the first and second inequalities hold for any operator norms and the last inequality is due to L-Lipschitzness of F.

Then it follows from the assumption that

$$\rho(\prod_{i=1}^{k} \nabla_{\mathbf{x}} F_{\mathcal{A}}(F^{i-1}(\mathbf{x}^*))) \leq L^k < \frac{1-\alpha}{\alpha}. \tag{65}$$

We conclude that G locally diffeomorphic, since $\rho(\prod_{i=1}^{k} \nabla_{\mathbf{x}} F(F^{i-1}(\mathbf{x}^*))) < \frac{1-\alpha}{\alpha}$ implies $0 \notin \mathrm{eig}(\nabla_{\mathbf{x}} G(\mathbf{x}))$.

Let us define the set of unstable equilibria of G as $U \stackrel{\text{def}}{=} \{\mathbf{x}^* : G(\mathbf{x}^*) = \mathbf{x}^*, \rho(\nabla_{\mathbf{x}} G(\mathbf{x}^*)) > 1\}$. Then it directly follows from the locally diffeomorphic G and the arguments of Lee et al. (2019); Daskalakis & Panageas (2018) that the set $\{x^{(0)} : \lim_{t\to\infty} G^t(x^{(0)}) \in U\}$ is of measure zero, which concludes the proof. We refer the readers to Appendix A of Daskalakis et al. (2018) for the detailed derivation of measure-zero arguments. □